NACA
Copy 135
RM L51D23

~~CONFIDENTIAL~~

NACA RM L51D23

TECH LIBRARY KAFB, NM
0069385

NACA

# RESEARCH MEMORANDUM

## THEORETICAL INVESTIGATION OF AN AUTOMATIC CONTROL SYSTEM WITH PRIMARY SENSITIVITY TO NORMAL ACCELERATIONS AS USED TO CONTROL A SUPERSONIC CANARD MISSILE CONFIGURATION

By Ernest C. Seaberg and Earl F. Smith

Langley Aeronautical Laboratory
Langley Field, Va.

19 Jy 1951
HEADQUARTERS
SPECIAL WEAPONS COMMAND
TECHNICAL LIBRARY

Declassified by Authority of (LARC) Security Classification Officer (SCO) Letter dated June 16, 1983
Marvin Johnson

[redacted]

This document contains classified information affecting the National Defense of the United States [redacted] meaning of the Espionage Act, USC 50:31 and 32. Its transmission or the [redacted] of its contents in any manner to an unauthorized person is prohibited by law.
Information so classified may be imparted only to persons in the military and naval services of the United States, appropriate civilian officers and employees of the Federal Government who have a legitimate interest therein, and to United States citizens of known loyalty and discretion who of necessity must be informed thereof.

NATIONAL ADVISORY COMMITTEE FOR AERONAUTICS
WASHINGTON
July 10, 1951

SWC 27,173

~~CONFIDENTIAL~~

5017

National Aeronautics and
Space Administration

Langley Research Center
Hampton, Virginia
23665

NASA

Reply to Attn of: 139A

JUN 16 1983

TO: Distribution

FROM: 180A/Security Classification Officer

SUBJECT: Authority to Declassify NACA/NASA Documents Dated Prior to January 1, 1960

Effective this date, all material (informal, correspondence) classified by this Center prior to January 1, 1960, is declassified. This action does not include material derivatively classified at the Center upon instructions from other Agencies.

Immediate re-marking is not required; however, until material is re-marked by lining through the classification and annotating with the following statement, it must continue to be protected as if classified:

> "Declassified by authority of LaRC Security Classification Officer (SCO) letter dated June 16, 1983," and the signature of person performing the re-marking.

If re-marking a large amount of material is desirable, but unduly burdensome, custodians may follow the instructions contained in NHB 1640.4, subpart F, section 1203.604, paragraph (h).

This declassification action complements earlier actions by the National Archives and Records Service (NARS) and by the NASA Security Classification Officer (SCO). In Declassification Review Program 807008, NARS declassified the Center's "Research Authorization" files, which contain reports, Research Authorizations, correspondence, photographs, and other documentation. Earlier, in a 1971 letter, the NASA SCO declassified all NACA/NASA formal series documents with the exception of the following reports, which must remain classified:

| Document No. | First Author |
|---|---|
| E-51A30 | Nagey |
| E-53G20 | Francisco |
| E-53G21 | Johnson |
| E-53K18 | Spooner |
| SL-54J21a | Westphal |
| E-55C16 | Fox |
| E-56H23a | Himmel |

JUN 23 1983

05-05-1997 11:29 804 864 2375 LARC TECH LIBRARY P.02

If you have any questions concerning this matter, please call Mr. William L. Simkins at extension 3281.

Jess G. Ross
2898

Distribution:
SDL 031

cc:
NASA Scientific and Technical
Information Facility
P.O. Box 8757
BWI Airport, MD 21240

NASA--NIS-5/Security
180A/RIAD
139A/TU&AO
139A/WLSimkins:elf 06/15/83 (3281)
139A/JS 6-15-83

31-01 HEADS OF ORGANIZATIONS
HESS, JANE S.,
MAIL STOP 185 BLDG 1194

TECH LIBRARY KAFB, NM
0069385



NATIONAL ADVISORY COMMITTEE FOR AERONAUTICS

RESEARCH MEMORANDUM

# THEORETICAL INVESTIGATION OF AN AUTOMATIC CONTROL SYSTEM WITH PRIMARY SENSITIVITY TO NORMAL ACCELERATIONS AS USED TO CONTROL A SUPERSONIC CANARD MISSILE CONFIGURATION

By Ernest C. Seaberg and Earl F. Smith

## SUMMARY

Results are presented of a theoretical investigation of an automatic control system with primary sensitivity to normal accelerations as used to control a specific supersonic canard missile. The acceleration control system consists of an integrating servomotor which receives its actuating signal from an accelerometer sensitive to the normal accelerations of the airframe being controlled. The servomotor operates the airframe control surfaces to obtain or maintain desired normal accelerations.

The analysis is based largely on comparisons of normal acceleration transient responses obtained for various conditions of Mach number, altitude, static margin, and rate-of-pitch feedback. The results indicate that the use of rate-of-pitch feedback and a high static margin with accompanying increase in integrating-servomotor gain and rapid control-surface deflection results in a more rapid transient response and a lower steady-state attitude error due to aerodynamic out-of-trim moment.

The acceleration control system appears to be a satisfactory method for obtaining longitudinal control of the supersonic airframe under consideration. This system has no directional space reference of its own, however, and its primary usefulness is therefore believed to be in conjunction with a homing seeker or with a guidance system which will provide a directional space reference.

## INTRODUCTION

As part of the general research program for investigating various means of automatic stabilization, the Pilotless Aircraft Research Division of the Langley Aeronautical Laboratory has been conducting a theoretical analysis to determine the possibilities of using an autopilot primarily sensitive to linear accelerations for longitudinal stabilization and control of a supersonic canard airframe. Physically this type of control combines the use of a linear accelerometer and servomotor to obtain desired normal accelerations of the missile. Since the acceleration control system has no directional space reference of its own, its primary usefulness is believed to be in conjunction with a homing seeker. An autopilot of the type investigated in this analysis is small, lightweight, and simple to fabricate as compared to a displacement-plus-rate type of autopilot. Longitudinal control through the use of an accelerometer also has the advantage of eliminating the problem of free gyroscope drift.

The analysis has been made for a specific supersonic canard missile configuration and is based mainly on flight conditions and stability characteristics anticipated as a result of previous flight tests of geometrically similar models. The results presented show the effects of the following conditions on the over-all performance of the autopilot-model combination:

(1) Static margin and Mach number variation

(2) The addition of a rate-of-pitch feedback control

(3) Altitude variation

(4) Aerodynamic out-of-trim moment

(5) Variation of servo-gain constants

(6) Mach number variation with fixed servo-gain constants

(7) The use of an accelerometer displaced ahead of model center of gravity to generate both normal-acceleration error and rate-of-pitch feedback signal.

## SYMBOLS

| | |
|---|---|
| $n_o$ | normal acceleration of airframe in g units |
| $n_i$ | desired normal acceleration of airframe in g units |
| $V_{n_o}$ | voltage proportional to $n_o$, volts |
| $V_{n_i}$ | voltage proportional to $n_i$, volts |
| $\epsilon$ | voltage error, volts $\left(\epsilon = V_{n_i} - V_{n_o}\right)$, or normal-acceleration error, g units $\left(\epsilon = n_i - n_o\right)$ |
| g | acceleration due to gravity, 32.2 feet per second per second |
| $\theta_o$ | pitch angle measured from the horizontal, degrees |
| $\dot{\theta}$ | first derivative of pitch angle with respect to time, degrees per second $(d\theta_o/dt)$ |
| $\alpha$ | angle of attack, degrees |
| $\dot{\alpha}$ | first derivative of angle of attack with respect to time, degrees per second $(d\alpha/dt)$ |
| $\gamma$ | flight-path angle, degrees $(\gamma = \theta - \alpha)$ |
| $\dot{\gamma}$ | first derivative of $\gamma$ with respect to time, degrees per second $(d\gamma/dt)$ |
| $\delta$ | canard control-surface deflection, degrees $\left(\delta = \delta_S - \delta_R\right)$ |
| $\delta_S$ | control-surface deflection due to integrating servo, degrees |
| $\delta_R$ | control-surface deflection due to rate servo, degrees |
| $\delta_{ot}$ | value of control-surface deflection which counterbalances out-of-trim moment, degrees |
| $K_1$ | integrating servo gain constant, radians per second per g |
| $K_R$ | rate-servo gain constant, radians per radian per second |

| | |
|---|---|
| $K_A$ | steady-state proportionality constant between voltage and acceleration, volts per g $\left[K_A = \left(\frac{V_{n_o}}{n_o}\right)_{\text{steady state}} = \frac{V_{n_1}}{n_1}\right]$ |
| t | time, seconds |
| M | Mach number |
| Y | stability axis which passes through center of gravity and is perpendicular to vertical plane of symmetry |
| $I_Y$ | moment of inertia about Y-axis, slug-feet square |
| $\bar{c}$ | mean aerodynamic chord, feet |
| c.p. | model center of pressure |
| SM | static margin, fraction of $\bar{c}$ |
| V | velocity, feet per second |
| m | mass, slugs |
| q | dynamic pressure, pounds per square foot; or $\frac{\dot{\theta}\bar{c}}{2V}$ (when used as a subscript) |
| S | wing area, square feet |
| $C_L$ | lift coefficient $\left(\frac{\text{Lift}}{qS}\right)$ |
| $C_m$ | pitching-moment coefficient $\left(\frac{\text{Pitching Moment}}{qS\bar{c}}\right)$ |
| $C_{L_\delta}$ | $\partial C_L/\partial\delta$ |
| $C_{L_\alpha}$ | $\partial C_L/\partial\alpha$ |
| $C_{m_\delta}$ | $\partial C_m/\partial\delta$ |
| $C_{m_\alpha}$ | $\partial C_m/\partial\alpha$ |
| $C_{m_{\dot{\alpha}}}$ | $\partial C_m/\partial\frac{\dot{\alpha}\bar{c}}{2V}$ |

| | |
|---|---|
| $C_{m_q}$ | $\partial C_m \Big/ \partial \frac{\dot{\theta}\bar{c}}{2V}$ |
| $j$ | $\sqrt{-1}$ |
| $\omega$ | angular frequency, radians per second |
| D | differential operator (d/dt) |
| s | Laplace transform variable corresponding to differential operator |
| KG | system or component transfer function; may be expressed as a function of $j\omega$, D, or s |
| AR | magnitude of $KG(j\omega)$ |
| PA | phase angle of $KG(j\omega)$ |
| R | Routh's discriminant |
| A,B,C,D,E,F | coefficients of the quintic characteristic equation of $\frac{n_o}{n_i}(s)$ |

## DESCRIPTION OF THE PROPOSED ACCELERATION CONTROL SYSTEM

The block diagram of the proposed acceleration control system with the airframe compensated by rate-of-pitch feedback is shown in figure 1. The voltage input $V_{n_i}$ of the system is made proportional to a desired normal acceleration $n_i$ of the airframe. The accelerometer produces a voltage $V_{n_o}$ proportional to the existing normal acceleration $n_o$ of the airframe. The proportionality constant $K_A$ between desired acceleration $n_i$ and input voltage $V_{n_i}$ is the same as the proportionality constant between existing acceleration $n_o$ and acceleration voltage $V_{n_o}$. Then if existing acceleration is not equal to desired acceleration an error signal $\epsilon$ excites the integrating servo. The integrating servo produces a control-surface deflection $\delta_s$ which is proportional to the integral of the error signal. This control surface deflection causes the airframe to turn in the proper direction to produce a normal-acceleration signal which tends to cancel the error signal. In the steady-state condition the error signal is zero, but the integral of the error, and hence the control-surface deflection, is not necessarily zero.

The effect of the rate servo can be thought of as a modification of the airframe response since its primary effect is to increase the damping ratio of the airframe.

Proposed configurations for the various elements, other than the airframe, are presented in the following paragraphs.

Rate servo.- The proposed rate servo consists of a rate gyro and hydraulic servo combined as shown schematically in figure 2(a). Figure 2 illustrates one possible mechanical arrangement, many variations of which are possible. If time lags and the effect of inertias are ignored, the control deflection $\delta_R$ is proportional to a rate input $\dot{\theta}$. For the present analysis, the rate servo was considered to be a single-degree-of-freedom, second-order system having a natural frequency of 88 radians per second and a damping ratio of 0.5. This is believed to be a conservative representation of the dynamic effects of an actual rate gyro plus servomotor.

Integrating servo.- A proposed integrating servo is shown schematically in figure 2(b). Since there are moving masses in this servo the response cannot be instantaneous as implied by the transfer function, $\frac{\delta}{\epsilon} = \frac{K_1}{s}$. However, the assumption made herein is that the fluid-supply pressure is high with no limit on the rate of flow, and the masses of the moving parts (including moving fluid) are small. Since such a servo is fast acting, the dynamic effects can be ignored for operation at low frequencies.

Accelerometer dynamics.- The term "accelerometer dynamics" as used here includes any dynamic effect between the normal acceleration $n_o$ of the airframe and the electrical accelerometer signal $V_{n_o}$. Most accelerometers having a range suitable for the present application have a natural frequency which is sufficiently high so that the dynamic effects of the accelerometer may be neglected; however, because of noise signals picked up by the accelerometer, the accelerometer signal may have to be filtered electrically. The dynamic effects of such a filter are included in the accelerometer dynamics discussed here.

For the major part of the present investigation, the effect of accelerometer dynamics was neglected; however, its effect was investigated for one set of conditions, and the results obtained are shown later. For this set of conditions, the following transfer function was used to represent the accelerometer dynamics.

$$\frac{V_{n_o}}{n_o} = \frac{24650}{D^2 + 314D + 24650}$$

This transfer function represents a second-order system having a natural frequency of 25 cycles per second and damping ratio of 1.0. At 5 cycles per second the amplitude ratio is 0.96 and the phase lag is 23°, and at 80 cycles per second the amplitude ratio is 0.1. This transfer function was used because it is believed that these phase and attenuation characteristics are representative of those to be expected from an actual accelerometer and filter suitable for the present application.

## METHOD OF ANALYSIS

The analysis is mainly concerned with obtaining the transient acceleration response $(n_o)$ to a unit-step acceleration input $(n_i)$. These responses are then used to determine the effect of variation of the automatic-control system gain constants and the airframe aerodynamic parameters. To facilitate analysis, the airframe and autopilot components can be represented by transfer functions which can be combined in block diagram form.

### Component Transfer Functions

Servomotor block.- This block represents an integrating servo. If the dynamics of the servomotor and control surface are neglected, this block can be drawn as:

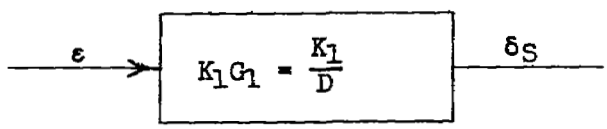


Airframe block.- The forms of the equations of motion for constant speed and disturbances from level flight are:

$$\left(\frac{I_Y}{qS\bar{c}} D^2 - C_{m_q} \frac{\bar{c}}{2V} D\right) \theta_o - \left(C_{m_\alpha} + C_{m_{\dot{\alpha}}} \frac{\bar{c}}{2V} D\right) \alpha = C_{m_\delta} \delta$$

$$\left(\frac{mV}{qS} D\right) \theta_o - \left(\frac{mV}{qS} D + C_{L_\alpha}\right) \alpha = C_{L_\delta} \delta$$

where the stability derivatives are expressed in radian measure.

Solution of these equations for $\frac{\theta_o}{\delta}$ gives the airframe transfer function, which can be represented in block diagram form as:

$$\xrightarrow{\delta} \boxed{K_2G_2 = \frac{a(D + b)}{D(D^2 + e\,D + f)}} \xrightarrow{\theta_o}$$

where

$$a = \frac{C_{m_\delta}\left(\frac{mV}{qS}\right) - C_{L_\delta}\left(C_{m_{\dot{\alpha}}}\frac{\bar{c}}{2V}\right)}{\left(\frac{I_Y}{qS\bar{c}}\right)\left(\frac{mV}{qS}\right)}$$

$$b = \frac{C_{m_\delta}C_{L_\alpha} - C_{m_\alpha}C_{L_\delta}}{C_{m_\delta}\left(\frac{mV}{qS}\right) - C_{L_\delta}\left(C_{m_{\dot{\alpha}}}\frac{\bar{c}}{2V}\right)}$$

$$e = \frac{C_{L_\alpha}}{\left(\frac{mV}{qS}\right)} - \frac{\left(C_{m_q} + C_{m_{\dot{\alpha}}}\right)\frac{\bar{c}}{2V}}{\left(\frac{I_Y}{qS\bar{c}}\right)}$$

$$f = -\frac{C_{L_\alpha}\left(C_{m_q}\frac{\bar{c}}{2V}\right) + C_{m_\alpha}\left(\frac{mV}{qS}\right)}{\left(\frac{I_Y}{qS\bar{c}}\right)\left(\frac{mV}{qS}\right)}$$

<u>The $n_o/\theta_o$ block.</u>- The transfer function $n_o/\theta_o$ is obtained from the relation

$$\frac{n_o}{\theta_o} = \frac{n_o/\delta}{\theta_o/\delta}$$

where

$$\frac{n_o}{\delta} = \frac{V}{32.2}\frac{\dot{\gamma}}{\delta}$$

and the function $\frac{\gamma}{\delta}$ is obtained by substituting $\alpha + \gamma$ for $\theta_o$ in the equations of motion. The solution for $\frac{\dot{\gamma}}{\delta}$ is then

$$\frac{\dot{\gamma}}{\delta} = \left(\frac{\gamma}{\delta}\right)D$$

For the case where $C_{L_\delta} = 0$, the transfer function $n_o/\theta_o$ in g units per radian can be represented in block-diagram form as:

$$\theta_o \longrightarrow \boxed{K_3G_3 = \frac{h\,D}{a(D + b)}} \longrightarrow n_o$$

where

$$h = \frac{V}{32.2}\,\frac{C_{m_\delta}\,C_{L_\alpha}}{\left(\frac{I_Y}{qS\bar{c}}\right)\left(\frac{mV}{qS}\right)}$$

and $a$ and $b$ are previously defined.

Rate-control block.- The rate control can be represented in block-diagram form as:

$$\theta_o \longrightarrow \boxed{K_RG_R = \frac{7744\,K_RD}{D^2 + 88D + 7744}} \longrightarrow \delta_R$$

This transfer function has been used previously in conjunction with a displacement autopilot in reference 1. The static sensitivity $(K_R)$ has the physical significance of being the magnitude of steady-state control-surface displacement $\delta_R$, resulting from a unit rate input $\dot{\theta}$.

Accelerometer block.- For the major part of this analysis, the dynamics of the accelerometer in the outside loop have been neglected. That is, the transfer function $\frac{V_{n_o}}{n_o}$ is assumed to be equal to unity. In determining the effect of including the accelerometer dynamics, it was assumed that the accelerometer and filter could be represented by the following block:

$$n_o \longrightarrow \boxed{K_AG_A = \frac{24650\,K_A}{D^2 + 314D + 24650}} \longrightarrow V_{n_o}$$

The gain $K_A$ was taken as unity since variations of $K_A$ have the same effect on the responses to an $n_i$ input as do variations of servo gain $K_1$, as can be derived by using the block diagram shown in figure 1.

## Method of Obtaining Transient Responses

The system analyses presented herein are based mainly on the transient responses of the system to a unit step input. Although such discontinuities in the input may never occur in practice, the responses to a unit step input are of value in making a comparison of a system's performance under various conditions.

The majority of the transient responses presented herein are square-wave responses obtained from plots of the closed-loop frequency response $\frac{n_o}{n_i}(j\omega)$ by the use of the following series:

$$n_o(t) = \left(\frac{AR}{2}\right)_{\omega=0} + \frac{2}{\pi} \sum_{m=1,3,5,\ldots} \frac{AR}{m} \sin\left(m\omega_1 t + PA\right)$$

where $n_o(t)$ is the response to a square-wave input. If the fundamental frequency $\omega_1$ of the square wave is made low enough so that the system transients die out in one-half period of the square wave, the square-wave reponse is essentially the response to a series of steps. Twelve terms of the above series were used and summed by a Fourier synthesizer. This instrument was developed by the Massachusetts Institute of Technology, and the mechanical and technical aspects of a similar instrument along with a description of the equipment and a derivation of the preceding series can be found in reference 2.

A graphical method employing the general theories of servomechanism analysis, as outlined in reference 3, was used to obtain the closed-loop frequency response prior to obtaining each transient. With the assumption made previously $\left(\frac{V_{n_o}}{n_o} = 1\right)$, the block diagram for the combination of automatic control system and model reduces to:

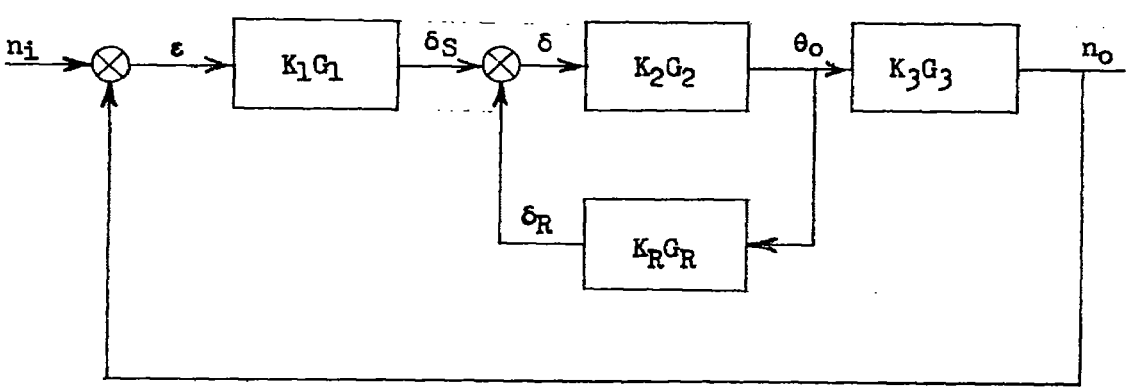

This analysis is mainly concerned with the transfer function $\frac{n_o}{n_i}$, from which the transient response $n_o(t)$ to a unit step $n_i$ can be obtained. As mentioned previously, a graphical method as described in reference 3 (chapter 8) is employed in obtaining $\frac{n_o}{n_i}$. Since the block diagram contains two feedback loops, the solution must be handled in two steps. The first step consists of obtaining an Lm-Angle plot of the open-loop response $\frac{\delta_R}{\delta}$, on which the M-N contours are superimposed. Then a satisfactory (but not necessarily optimum) adjustment of the rate servo gain constant $K_R$ can be made and the closed-loop response $\frac{\delta_R}{\delta_S}$ obtained. The second step combines the inner loop with the remaining components of the block diagram to obtain the Lm-Angle plot of the open-loop response $\frac{n_o}{\epsilon}$, on which the M-N contours are also superimposed. The integrating servo gain constant $K_I$ is adjusted on this plot. The significance of this adjustment is that it fixes the peak amplitude ratio of the closed-loop $\frac{n_o}{n_i}(j\omega)$. In most cases, the value of $K_I$ was chosen, as suggested in references 3 and 4, so that

$$\left| \frac{n_o}{n_i}(j\omega) \right|_{max} = 1.3$$

## RESULTS AND DISCUSSION

The results which follow show the effect of varying the airframe static margin, flight conditions, and autopilot gain constants on the over-all performance of the combination of the automatic-control system and model using a specific supersonic airframe. A photograph and plan-view sketch of the airframe are shown in figure 3. Flight tests of geometrically similar airframes have previously been conducted, the results of which are presented in references 5, 6, and 7. The estimated and measured longitudinal derivatives given in table I are based on reference 6, in which the model center of gravity was 73.53 inches behind the nose. The measured derivatives for intermediate static-margin values were taken directly from this reference, and the values given for small and large static margins were obtained from the estimated changes of the measured derivatives due to shifts in the airframe center of gravity. The static margin varies with Mach number in each static-margin category listed in table I. The values given for intermediate static margin, for example, vary from $0.333\bar{c}$ to $0.294\bar{c}$ as $M$ varies between 1.0 and 2.0. This variation is due to shifts in the airframe center of pressure with Mach number. The variations of the standard atmosphere flight conditions used in this analysis are given in table II.

Effect of static margin and Mach number variation.- The transient responses ($n_o$ to a unit step acceleration input) shown in figures 4, 5, and 6 are for small, intermediate, and large static margins, respectively. On these figures, the value of the rate-servo gain constant ($K_R$) was chosen such that the value of the peak amplitude ratio of the transfer function $\frac{\delta_R}{\delta_S}(j\omega)$ was equal to 1.3 and the value of the integrating-servo gain constant $K_1$ was chosen such that the peak amplitude ratio of the closed-loop frequency response $\frac{n_o}{n_1}(j\omega)$ was also equal to 1.3. An examination of figures 4, 5, and 6 reveals that the response time (the time required for the output transient to reach and remain within a given percent of steady state) is decreased by increasing either static margin or Mach number. The most rapid responses obtained are shown in figure 6 which is based on sea-level flight of the model with large static margin.

Effect of rate-of-pitch feedback.- Some of the responses shown in figures 4, 5, and 6 are for $K_R = 0$; setting $K_R$ equal to zero has the effect of removing the rate-servo block (see fig. 1). An example of the effect of rate-of-pitch feedback is best shown by referring to figure 5 where the system transient response for $K_R = 0$ is shown along with responses including $\dot{\theta}$ feedback for each Mach number. An examination of the responses shown in this figure indicates that including $\dot{\theta}$ feedback in this type of control system has the effect of increasing the damping of the missile and allows an increase in the integrating-servo gain constant $K_1$, which results in a faster response.

As mentioned in the section METHOD OF ANALYSIS, the transient responses were obtained by the use of a Fourier synthesizer. A comparison between a Fourier synthesizer result and a transient response calculated by the methods of Laplace (references 3 and 8) is made in figure 7 for the case of sea-level flight at $M = 1.6$ and with $SM = 0.294\bar{c}$. Other comparisons of the results obtained by these two methods have been made and agreement between the two methods is considered sufficient to justify use of the Fourier synthesizer to obtain the transient responses.

Effect of altitude variation.- Except for altitude and servo-gain adjustments, the responses shown in figure 5(c) are for the same conditions as those presented in figure 8 where the $n_o$ transient responses to a unit step acceleration input are based on flight at 10,000 feet and 40,000 feet. The values of $K_1$ and $K_R$ used in figure 8 (except for the dotted curve of figure 8(a)) were chosen such that the peak amplitude ratios of the transfer functions $\frac{\delta_R}{\delta_S}(j\omega)$ and $\frac{n_o}{n_1}(j\omega)$ were equal to 1.3. As is shown, flight at 10,000 feet produces a somewhat

slower response than that obtained at sea level while flight at 40,000 feet shows a considerable increase in the normal acceleration response time. A comparison of figure 5(c) and figure 8(a) indicates that the value of these servo gain constants did not change appreciably between sea level and 10,000 feet. The dotted curve of figure 8(a) is the response at 10,000 feet with rate-of-pitch feedback using the same servo gain adjustments that were used to obtain the sea-level response of figure 5(c). Since these responses do not differ greatly, it is believed that a fair approximation of the behavior of the airframe between sea level and 10,000 feet is obtained by basing the analysis entirely on sea-level flight.

Effect of accelerometer dynamics.- As mentioned previously in the description of the proposed acceleration control system, the accelerometer dynamics can be represented by the transfer function

$$\frac{V_{n_o}}{n_o} = \frac{24650}{D^2 + 314D + 24650}$$

In figure 1, this transfer function is labeled "accelerometer dynamics" in the outer feedback loop. In figure 9, a comparison is made of the response obtained by using the proposed acceleration control system with and without the accelerometer dynamics included in the outer feedback loop. The curves shown in figure 9 are based on sea-level flight at $M = 1.6$ and with $SM = 0.294\bar{c}$, and the results indicate that a slight increase in response time and period of the transient oscillations is obtained with the inclusion of accelerometer dynamics. On this basis, using the simplifying assumption that $\frac{V_{n_o}}{n_o} = 1$ for the major part of this analysis seems to be justified.

Effect of aerodynamic out-of-trim moment.- In the automatic control system being investigated, an aerodynamic out-of-trim moment can be represented by an equivalent control-surface deflection, to be denoted

by $\delta_{ot}$. This control-surface deflection can be represented in the system block diagram as an additional input as follows:

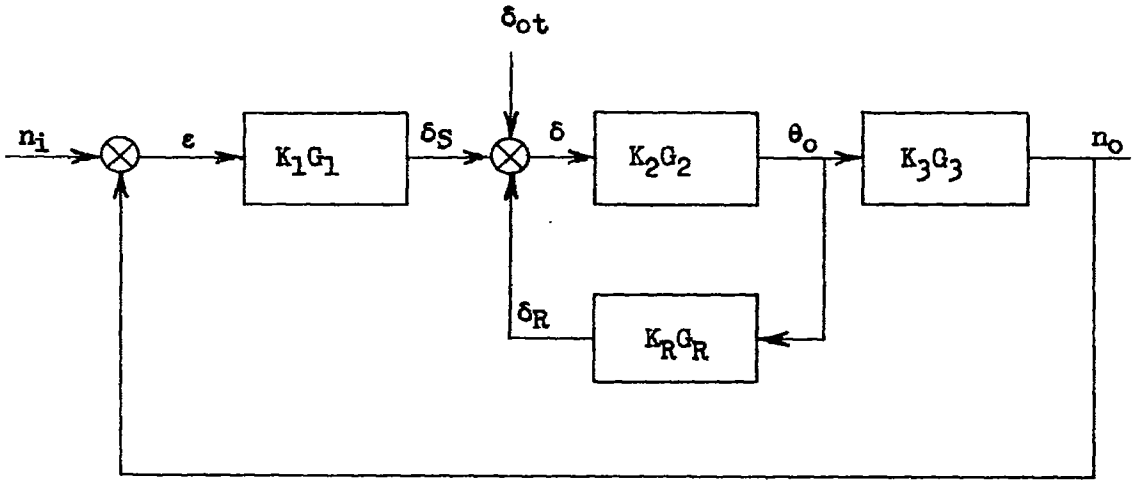


The transfer function $\frac{n_o}{\delta_{ot}}$ can be derived by setting $n_i = 0$ and employing the relations

$$n_o = -\epsilon$$

and

$$\delta = \delta_S - \delta_R + \delta_{ot}$$

Using the general theories of servomechanism analysis, the transfer function $\frac{n_o}{\delta_{ot}}$ is:

$$\frac{n_o}{\delta_{ot}} = f(s) = \frac{K_2G_2K_3G_3}{1 + K_1G_1K_2G_2K_3G_3 + K_2G_2K_RG_R} \tag{1}$$

The steady-state $n_o$ error is then obtained by applying the final-value theorem (see reference 3, chapter 3) to equation (1) as follows:

$$\lim_{t \to \infty} n_o(t) = \lim_{s \to 0} s \left[\frac{\delta_{ot}}{s} f(s)\right]$$

from which it is found that $\frac{n_o}{\delta_{ot}}$ (steady state) is always zero for the control system under consideration.

Similarly, the transfer function $\frac{\theta_o}{\delta_{ot}}$ can be derived as

$$\frac{\theta_o}{\delta_{ot}} = \frac{K_2G_2}{1 + K_1G_1K_2G_2K_3G_3 + K_2G_2K_RG_R} \tag{2}$$

Then by applying the final-value theorem, $\frac{\theta_o}{\delta_{ot}}$ (steady state) is found to be finite, the value of which is a measure of the effect of out-of-trim moment.

The results of the out-of-trim investigation conducted herein are presented in table III where the values of $\frac{\theta_o}{\delta_{ot}}$ (steady state) are tabulated for the automatic stabilization system with and without rate-of-pitch feedback. The results show that the system with rate feedback produces less $\theta_o$ error due to $\delta_{ot}$ for any set of comparable conditions. It is also shown that the magnitude of the error increases with increasing Mach number and decreases with increasing static margin. These results indicate that the use of rate feedback and high static margin will keep the $\theta_o$ error due to out-of-trim moment at a minimum. To summarize, the principal effect of an aerodynamic out-of-trim moment is to cause a steady-state error in pitch angle $\theta_o$, with no steady-state error in normal acceleration.

Application of Routh's discriminant to the stability analysis.- An application of Routh's criterion for the case of sea-level flight at $M = 1.6$ with $SM = 0.294\bar{c}$ is presented in figure 10. The characteristic equation of the closed-loop transfer function $\frac{n_o}{n_i}(s)$ with rate-of-pitch feedback is of fifth degree. The conditions for complete stability for a system having a characteristic equation of fifth degree are derived in reference 9, and applications of Routh's criterion including the necessary and sufficient conditions for complete stability are given in reference 10.

In conducting the analysis based on Routh's criterion as presented herein, the coefficients of the characteristic stability equation were expressed as functions of $K_1$ and $K_R$. The curve presented in figure 10 was then obtained from the condition for neutral oscillatory stability

$$R = (BC - AD)(DE - CF) - (BE - AF)^2 = 0$$

Any combination of the values of $K_R$ and $K_1$ falling above the neutral oscillatory stability boundary in figure 10 produces oscillatory instability. The lower stability limit of the integrating servo gain $K_1$ was determined from the coefficient F which is a constant multiplied by $K_1$. Therefore, since an unstable root would exist if $K_1$ assumed a negative value, the lower limit for $K_1$ is zero. Since the other conditions for complete stability as given in reference 10 fall outside but indicate stability in the direction of the stable region of figure 10, any set of values of $K_1$ and $K_R$ falling within this region will produce a stable system.

Effect of varying rate-servo gain constant $(K_R)$.- A locus of points based on six values of $K_R$ and for which $K_1$ was adjusted to make the peak-amplitude ratio of the transfer function $\frac{n_o}{n_i}(j\omega)$ equal to 1.3 is shown in figure 10. Closed-loop frequency responses $\frac{n_o}{n_i}(j\omega)$ based on values of $K_1$ and $K_R$ which correspond to the points of this locus and based on the same flight conditions used in figure 10 are presented in figure 11. In figure 12, the transient responses ($n_o$ to a unit step $n_i$) obtained from each frequency response are shown. The results given in figure 11 indicate that the resonant frequency peak occurs at a higher frequency as $K_R$ is decreased, and as the value of $K_R$ approaches zero a dip, or bucket, appears in the lower frequency range of the amplitude-ratio curves. In figure 12, a slight decrease in the transient response time is shown as $K_R$ decreases; however, for the case of $K_R = 0$, a slowly rising oscillatory transient response, resulting principally from the low frequency characteristics of the frequency response, is obtained as shown by the final plot. The foregoing data indicate that values of $K_R$ in the range 0.062 to 0.049 yield satisfactory responses in that they are rapid and well damped, although the exact adjustment of $K_R$ does not seem to be critical if $K_1$ is adjusted to obtain a slight overshoot of the $n_o$ transient response.

Effect of varying Mach number with servo gains fixed.- The effect of fixing the values of the servo gain constants and varying the Mach number is shown for intermediate and large static margins in figures 13 and 14, respectively. The curves presented in these figures are based on sea-level flight at four different Mach numbers and show the normal acceleration responses obtained when $K_1$ and $K_R$ are fixed at the values shown in figure 15 at $M = 1.6$.

The variations of $K_R$ and $K_1$ with Mach number shown in figure 15 are based on the values of these gain constants used previously in obtaining the responses shown in figures 5 and 6 where the peak amplitude ratio of $\frac{n_o}{n_i}(j\omega)$ was set at 1.3. It is shown in figures 13 and 14

that, when $K_1$ is adjusted to give $\left|\frac{n_o}{n_i}(j\omega)\right|_{max} = 1.3$ at $M = 1.6$, values of $M$ less than 1.6 give more stable responses and the $n_o$ transient response becomes more oscillatory as $M$ is increased above 1.6. The oscillatory response obtained for $M = 2.0$ in figure 14 indicates that the effect of varying Mach number with servo gains fixed is greater with large static margin.

The use of an auxiliary control to vary the servomotor gains with Mach number to conform with the values given in figure 15 would reduce the effect of Mach number variation. Since it has already been shown that the exact adjustment of $K_R$ is not critical if $K_1$ is adjusted to obtain a slight overshoot of the $n_o$ transient response, the design of a gain-varying device could be simplified by basing it only on the variation of $K_1$ with Mach number.

Transient responses of $\theta_o$, $\alpha$, $\gamma$, and $\delta$ to a unit step acceleration input.- The results presented in figure 16 are based on sea-level flight at $M = 1.6$ for two values of static margin. Figure 16(a) is for $SM = 0.294\bar{c}$, whereas figure 16(b) is for $SM = 0.564\bar{c}$. Normal-acceleration transient responses to a unit step acceleration input for the same conditions as used in obtaining the responses of figure 16 have previously been shown in figures 5(c) and 6(c). It can be seen in figure 16 that the angle of attack approaches a steady-state value of approximately $0.23^\circ$ per $g$ normal acceleration for either value of static margin, and after 0.3 second the steady-state rate of change of pitch angle and flight-path angle is approximately $1^\circ$ per second per $g$. An examination of the control-surface-deflection ($\delta$) responses presented in figure 16 shows that, as would be expected, approximately twice as much steady-state $\delta$ is required per $g$ normal acceleration with the larger static margin; namely, $0.49^\circ$ per $g$ for $SM = 0.564\bar{c}$ and $0.255^\circ$ per $g$ for $SM = 0.294\bar{c}$.

A further examination of figures 16(a) and 16(b) shows that more rapid missile responses are obtained with high static margin. This result is obtained because the increased aerodynamic stability of the airframe allows a higher integrating-servo gain $K_1$, which produces a more rapid change in control-surface deflection.

Gravitational influence.- The results of this analysis can be applied either to pitch or to yaw due to the symmetry of the airframe in these planes. However, in pitch, because of the 1 g acceleration due to gravity, there exists a gravitational influence on the accelerometer which varies as $\cos \theta_o$. This influence has been neglected throughout this analysis. Its omission is not believed to affect the transient responses seriously since the total variation of $\theta_o$ during the transient response time is small, as can be seen in figure 16. The

effect of this gravitational influence on the trim condition is not serious because in practice the trim condition will be continuously dictated by a homing seeker or other guidance system.

System responses obtained with accelerometer placed ahead of center of gravity to generate rate-of-pitch feedback signal.- In practice, it may be desirable to include only one servo in the system and add the normal-acceleration and rate-of-pitch signals electrically or by some other method. Mr. H. D. Garner of the Instrument Research Division at the Langley Laboratory has suggested that the rate-of-pitch feedback may be obtained by mounting the normal accelerometer ahead of the center of gravity of the airframe so that the accelerometer will be sensitive to angular acceleration $\ddot{\theta}$ as well as normal acceleration $n_o$. Since the accelerometer signal is fed through the integrating servo, the component due to angular acceleration is effectively an angular-rate feedback or rate-of-pitch feedback.

The rate-of-pitch feedback gain is then determined by the distance from the center of gravity of the airframe to the normal accelerometer. With static margin of $0.294\bar{c}$ and $M = 1.6$, to obtain the response of figure 5(c) (with $K_1 = 0.11$ and $K_R = 0.062$), the normal accelerometer must be mounted 18.1 feet ahead of the airframe center of gravity. With static margin of $0.564\bar{c}$ and $M = 1.6$, to obtain the response of figure 6(c) (with $K_1 = 0.21$ and $K_R = 0.047$), the normal accelerometer must be mounted 7.2 feet ahead of the airframe center of gravity. The size of the airframe used in this investigation limits the distance between airframe center of gravity and normal accelerometer to a maximum of about 5 feet.

A theoretical investigation of the system response with the normal accelerometer mounted 5 feet ahead of the airframe center of gravity with static margin of $0.564\bar{c}$ and $K_1 = 0.09$ (effective $K_R = 0.014$) was made for Mach numbers of 1.0, 1.2, 1.6, and 2.0. The results are shown in figure 17. It can be seen from figure 17 that this location of the accelerometer does not provide enough effective pitch-rate feedback to damp the system satisfactorily.

To produce sufficient damping by this method, it would be necessary to extend the nose of the model 2 feet or more. An alternative is to use two normal accelerometers, one mounted a distance $l$ ahead of the airframe center of gravity and one mounted on the airframe center of gravity. The signals from these accelerometers are subtracted before being fed to the integrating servo. The pitch-rate feedback gain and the acceleration feedback gain can then each be adjusted independently for any distance $l$ by adjusting independently the two accelerometer gains and the integrating servo gain. It is believed that no difficulty will be encountered due to slight mismatching of the dynamics of the

two accelerometers since the accelerometer natural frequencies will be considerably higher than the resonant frequency of the system and since the high frequency components of the accelerometer signals will be attenuated by the integrating servo.

Comparison of acceleration control system with an attitude control system.- A reasonable way to compare two control systems to be used for missile guidance is to compare their effectiveness in obtaining rapid changes in flight-path direction without producing excessive normal accelerations of the airframe. This comparison has been made between the acceleration control system analyzed herein and the attitude control system analyzed in reference 1; the results are shown in figure 18. The results for the acceleration control system and for the attitude control system were compared at a Mach number of 1.6 and 1.8, respectively, because these results were available. The static margins used were considered to produce the most satisfactory results for each of the two systems, that is, intermediate static margin for the acceleration control and small static margin for the attitude control. In figure 18, the command input $\theta_i$ to the attitude control system is a one-degree step. As is shown, this produces a peak normal acceleration of 4.1g and results in a steady-state change in flight-path angle $\gamma$ of $1^{\circ}$. The $\gamma$ transient has died out to within 5 percent of its final value in approximately 0.86 seconds. The command input to the acceleration control system is a square pulse. The magnitude of the square pulse was chosen so as to produce a peak normal acceleration of 4.1g and the time duration was chosen to produce a steady-state change in flight-path angle $\gamma$ of $1^{\circ}$. As shown in figure 18, the $\gamma$ transient has died out to within 5 percent of its final value in approximately 0.45 second or approximately one-half the time required by the attitude control system. This result indicates that changes in flight-path direction may be obtained more rapidly with the acceleration control system.

The areas under each of the normal-acceleration-response curves shown in figure 18 are approximately equal. Since the normal acceleration is proportional to angle of attack, there is no apparent increase in velocity loss due to drag in obtaining the shorter $\gamma$ response time with the acceleration control system. The comparison made here is based on the available data for the attitude control system. It is believed that more cases and other variables would have to be considered before a general conclusion as to the relative merit of either system can be made.

## CONCLUSIONS

The acceleration control system is primarily sensitive to normal accelerations of the airframe and actuates the control surfaces through the use of an integrating servomotor to obtain desired normal accelerations. An automatic control system with primary sensitivity to linear acceleration appears to be a satisfactory method for obtaining longitudinal control of the supersonic airframe under consideration. The acceleration control system, however, has no directional space reference of its own; therefore it is believed that the primary usefulness of such a system is in conjunction with a homing seeker or with a guidance system which will provide a directional space reference. The conclusions reached as a result of the analyses presented herein, based on a specific supersonic airframe configuration, are as follows:

1. On the basis of a comparison of the normal-acceleration transient responses presented herein for various Mach numbers, static margins, and altitudes, it can be concluded that:

(a) Increasing the airframe static margin produces more rapid transient responses, which may necessitate the use of a fast-acting servomotor.

(b) Including rate-of-pitch feedback in the automatic control system has the effect of increasing the damping of the missile and allows an increase in the integrating-servo gain constant resulting in a more rapid response. The exact adjustment of the rate-of-pitch feedback control gain constant does not seem to be critical if the integrating-servo gain is adjusted to obtain a slight overshoot of the normal-acceleration transient response.

(c) More rapid transient responses can be obtained with higher Mach number.

(d) Flight at altitude produces slower responses than those obtained at sea level; however, a fair approximation of the behavior of the system between sea level and 10,000 feet is obtained by basing the analysis entirely on sea-level flight.

2. When the integrating-servomotor gain constant is adjusted so that the peak amplitude ratio of the system-closed-loop transfer function is 1.3 at a Mach number of 1.6, flight at lower Mach numbers yields more stable transient responses and the system transient response becomes more oscillatory as the Mach number is increased above 1.6. The effect of varying Mach number with fixed servomotor gain constants is greater with large static margin.

3. The principal effect of an aerodynamic out-of-trim moment is to cause a steady-state error in pitch angle with no steady-state error in normal acceleration. The use of a rate-of-pitch feedback control and high static margin tends to minimize the steady-state error in pitch angle due to an aerodynamic out-of-trim moment of the airframe.

4. A comparison between the acceleration control system and an attitude control system indicates that changes in flight-path direction may be obtained more rapidly with the acceleration control system with no apparent increase in velocity loss due to drag.

5. Theoretically, effective rate-of-pitch feedback may be obtained in a system employing an integrating servomotor by using a normal accelerometer mounted ahead of the model center of gravity; thus the necessity of a rate gyro in the control system may be eliminated.

Langley Aeronautical Laboratory
National Advisory Committee for Aeronautics
Langley Field, Va.

REFERENCES

1. Nelson, Walter C., and Passera, Anthony L.: A Theoretical Investigation of the Influence of Auxiliary Damping in Pitch on the Dynamic Characteristics of a Proportionally Controlled Supersonic Canard Missile Configuration. NACA RM L50F30, 1950.

2. Seamans, Robert C., Jr., Bromberg, Benjamin G., and Payne, L. E.: Application of the Performance Operator to Aircraft Automatic Control. Jour. Aero. Sci., vol. 15, no. 9, Sept. 1948, pp. 535-555.

3. Brown, Gordon S., and Campbell, Donald P.: Principles of Servomechanisms. John Wiley & Sons, Inc., 1948.

4. Hall, Albert C.: The Analysis and Synthesis of Linear Servomechanisms. The Technology Press, M.I.T., 1943, chs. 3 and 4.

5. Gardiner, Robert A., and Zarovsky, Jacob: Rocket-Powered Flight Test of a Roll-Stabilized Supersonic Missile Configuration. NACA RM L9K01a, 1950.

6. Zarovsky, Jacob, and Gardiner, Robert A.: Flight Investigation of a Roll-Stabilized Missile Configuration at Varying Angles of Attack at Mach Numbers between 0.8 and 1.79. NACA RM L50H21, 1950.

7. Niewald, Roy J., and Moul, Martin T.: The Longitudinal Stability, Control Effectiveness, and Control Hinge-Moment Characteristics Obtained from a Flight Investigation of a Canard Missile Configuration at Transonic and Supersonic Speeds. NACA RM L50I27, 1950.

8. Churchill, Ruel V.: Modern Operational Mathematics in Engineering. McGraw-Hill Book Co., Inc., 1944.

9. Routh, Edward John: Dynamics of a System of Rigid Bodies. Part II. Sixth ed., rev. and enl., Macmillan and Co., Ltd., 1905, pp. 223-230.

10. Sternfield, Leonard: Effect of Automatic Stabilization on the Lateral Oscillatory Stability of a Hypothetical Airplane at Supersonic Speeds. NACA TN 1818, 1949.

TABLE I

LONGITUDINAL DERIVATIVES

[All derivatives in radian measure; $I_Y$ = 31.3 slug-ft$^2$; m = 5.05 slugs; $\bar{c}$ = 1.776 ft; S = 4.1 sq ft]

| Mach number | SM (fraction of $\bar{c}$) | $C_{m_q}$ | $C_{m_\alpha}$ | $C_{m_\delta}$ | $C_{m_{\dot{\alpha}}}$ | $C_{L_\delta}$ | $C_{L_\alpha}$ |
|---|---|---|---|---|---|---|---|
| Estimated derivatives for small static margin (static margin = 2 inches at M = 1.6) | | | | | | | |
| 1.0 | 0.126 | -6.55 | -0.406 | 0.797 | -0.730 | 0 | 3.22 |
| 1.2 | .134 | -6.96 | -.404 | .820 | -.770 | 0 | 3.02 |
| 1.6 | .094 | -6.68 | -.245 | .702 | -.740 | 0 | 2.61 |
| 2.0 | .042 | -6.61 | -.104 | .573 | -.730 | 0 | 2.46 |
| Measured derivatives for intermediate static margin (static margin = 6.27 inches at M = 1.6) | | | | | | | |
| 1.0 | 0.333 | -6.97 | -1.07 | 0.797 | -0.774 | 0 | 3.22 |
| 1.2 | .339 | -7.48 | -1.025 | .820 | -.831 | 0 | 3.02 |
| 1.6 | .294 | -7.22 | -.763 | .702 | -.802 | 0 | 2.61 |
| 2.0 | .249 | -6.39 | -.613 | .573 | -.717 | 0 | 2.46 |
| Estimated derivatives for large static margin (static margin = 12 inches at M = 1.6) | | | | | | | |
| 1.0 | 0.601 | -8.13 | -1.94 | 0.797 | -0.903 | 0 | 3.22 |
| 1.2 | .606 | -8.88 | -1.83 | .820 | -.987 | 0 | 3.02 |
| 1.6 | .564 | -8.47 | -1.47 | .702 | -.941 | 0 | 2.61 |
| 2.0 | .516 | -7.43 | -1.27 | .573 | -.826 | 0 | 2.46 |

NACA

TABLE II

VARIATION OF FLIGHT CONDITIONS

| Altitude (ft) | Mach number | q (lb/sq ft) | V (ft/sec) |
|---|---|---|---|
| Sea level | 1.0 | 1481 | 1116 |
| Sea level | 1.2 | 2132 | 1339 |
| Sea level | 1.6 | 3791 | 1785 |
| Sea level | 2.0 | 5980 | 2245 |
| 10,000 | 1.6 | 2602 | 1721 |
| 40,000 | 1.6 | 702 | 1553 |

TABLE III

STEADY-STATE $\theta_o$ ERROR DUE TO $\delta_{ot}$

| Mach Number | SM (fraction of $\bar{c}$) | Altitude (ft) | $\frac{\theta_o}{\delta_{ot}}$ (steady state) |
|---|---|---|---|
| Without rate-of-pitch feedback | | | |
| 1.0 | 0.126 | Sea level | 1.62 |
| 1.2 | .134 | ---do---- | 1.45 |
| 1.6 | .094 | ---do---- | 2.96 |
| 2.0 | .042 | ---do---- | 5.86 |
| 1.0 | .333 | ---do---- | 0.8 |
| 1.2 | .339 | ---do---- | .8 |
| 1.6 | .294 | ---do---- | .9 |
| 2.0 | .249 | ---do---- | .96 |
| 1.6 | .564 | ---do---- | .53 |
| 1.6 | .294 | 10,000 | .93 |
| 1.6 | .294 | 40,000 | .69 |
| With rate-of-pitch feedback | | | |
| 1.6 | 0.094 | Sea level | 1.08 |
| 2.0 | .042 | ---do---- | 2.15 |
| 1.0 | .333 | ---do---- | 0.13 |
| 1.2 | .339 | ---do---- | .16 |
| 1.6 | .294 | ---do---- | .17 |
| 2.0 | .249 | ---do---- | .21 |
| 1.0 | .601 | ---do---- | .073 |
| 1.2 | .606 | ---do---- | .075 |
| 1.6 | .564 | ---do---- | .085 |
| 2.0 | .516 | ---do---- | .096 |
| 1.6 | .294 | 10,000 | .16 |
| 1.6 | .294 | 40,000 | .20 |

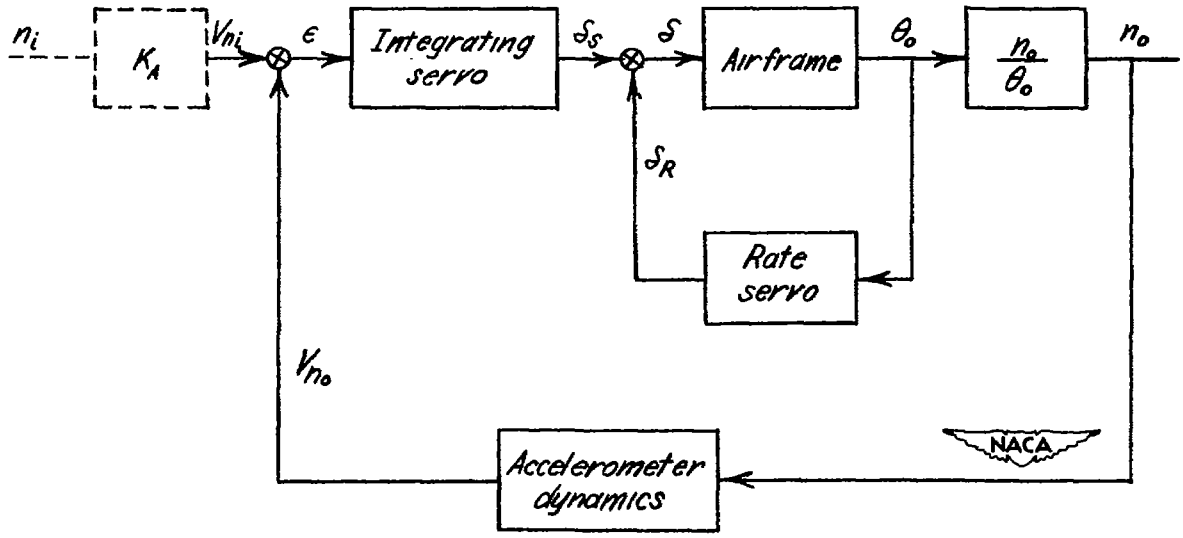


Figure 1.- Block diagram of the proposed acceleration control system.

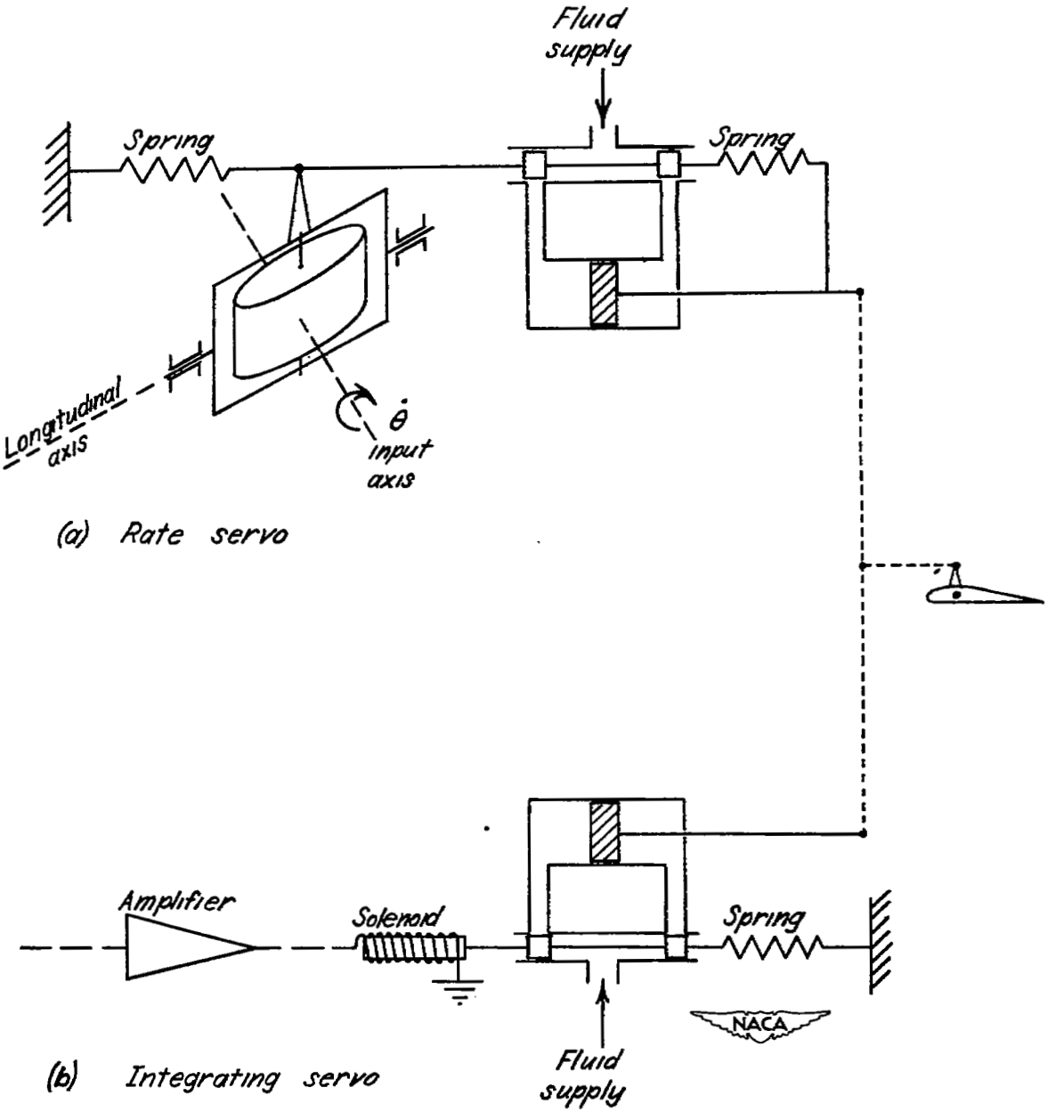


Figure 2.- Schematic diagram of proposed rate servo and integrating servo illustrating a possible mechanical arrangement.

CONFIDENTIAL

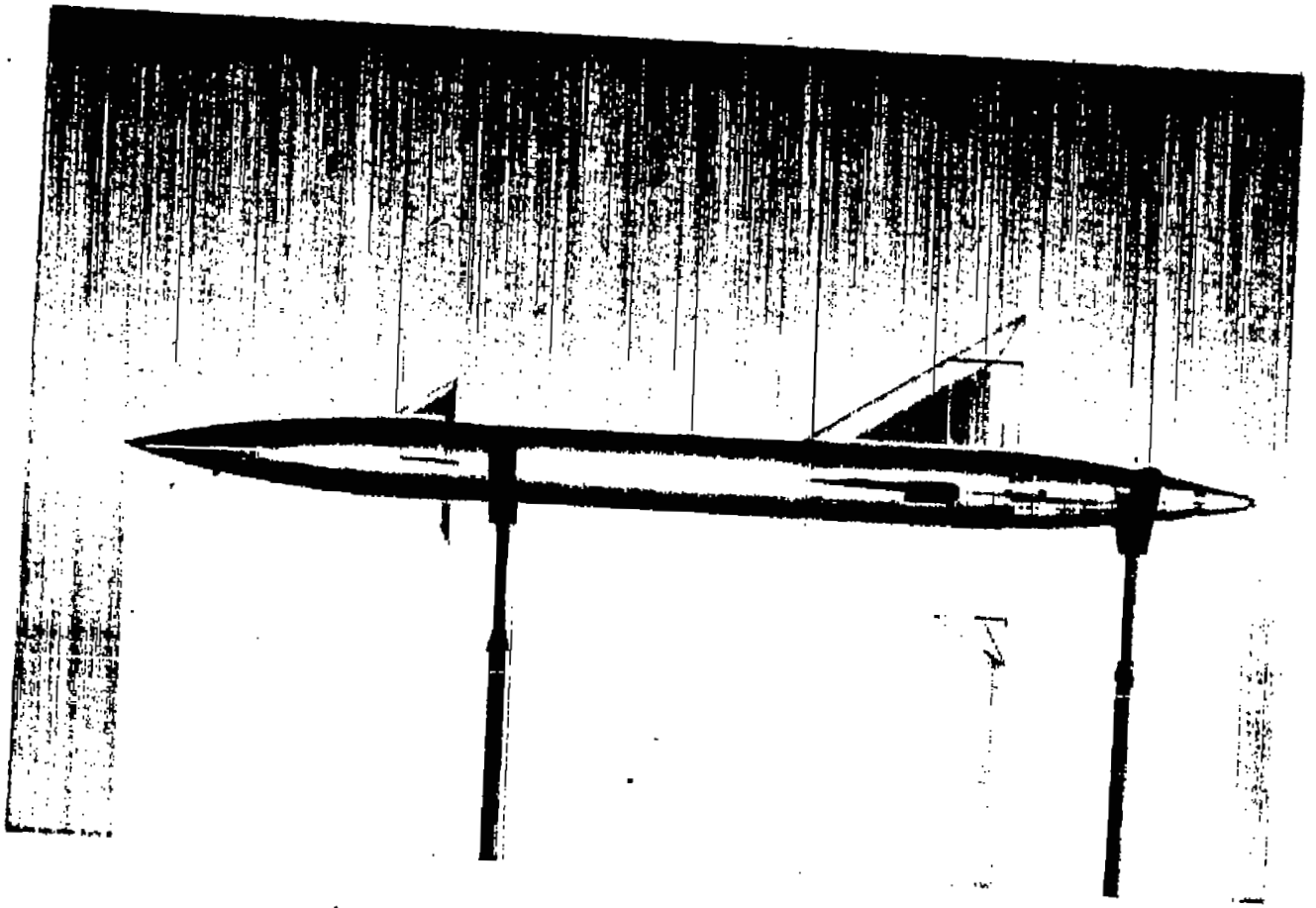

(a) Photograph of model configuration.

Figure 3.- Supersonic missile research model configuration.

CONFIDENTIAL

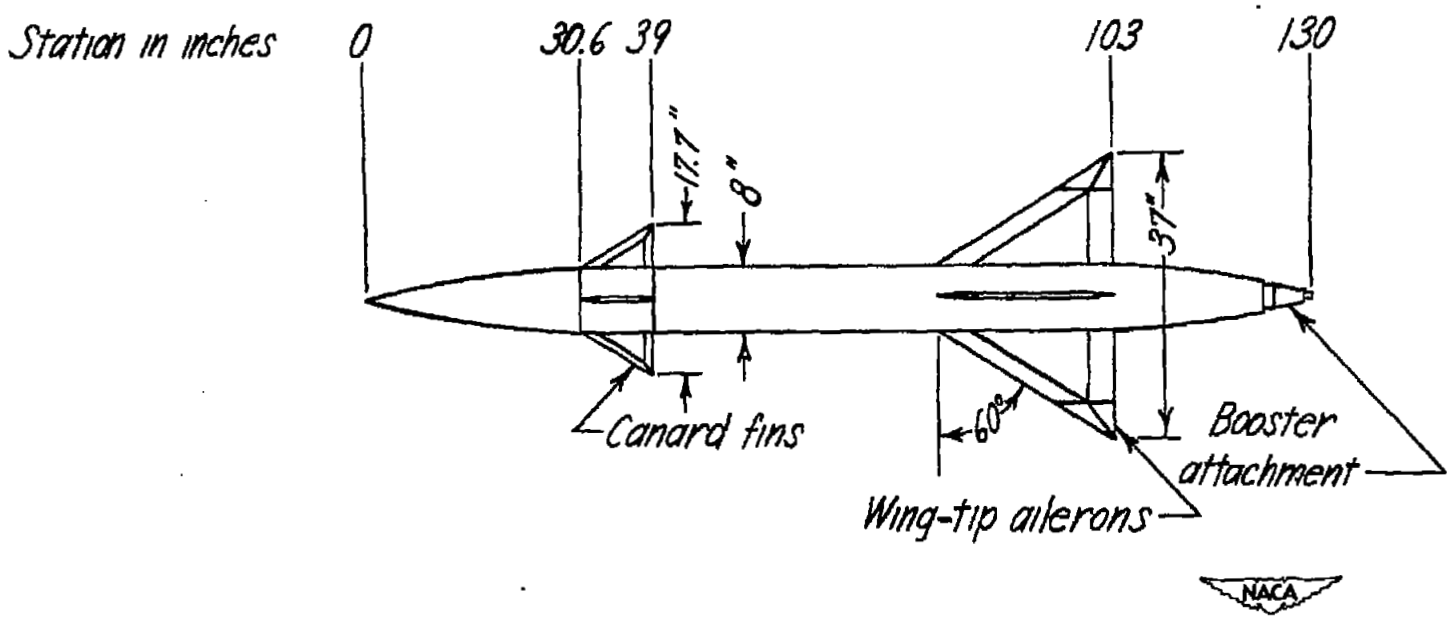


| c.p. location (station) | Mach number |
|---|---|
| 80.64 | 1.0 |
| 80.74 | 1.2 |
| 79.84 | 1.6 |
| 78.83 | 2.0 |

(b) Plan-view sketch of model configuration.

Figure 3.- Concluded.

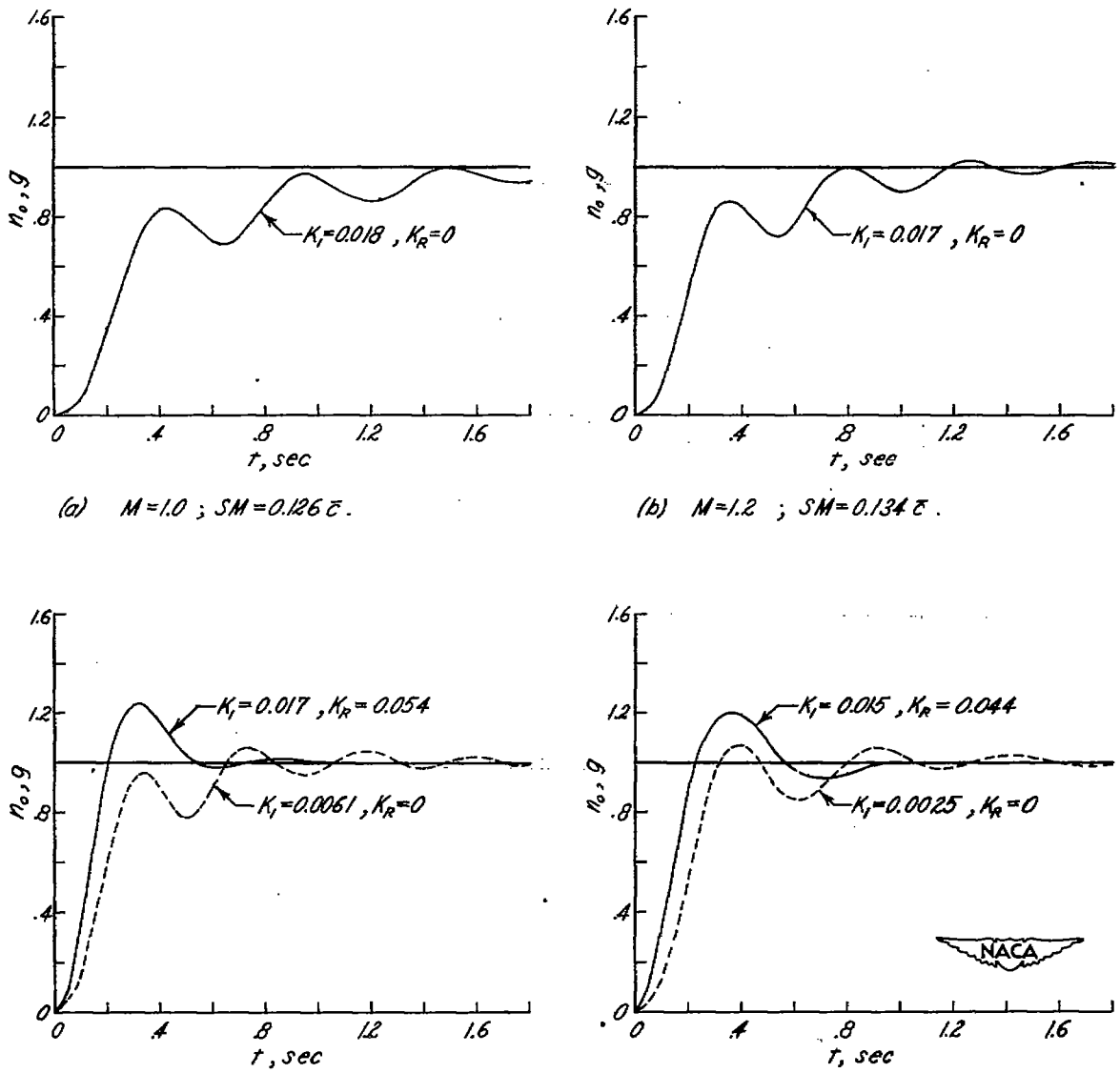


Figure 4.- Normal acceleration ($n_o$) responses to a unit step acceleration input ($n_i$) for various Mach numbers based on sea-level flight of the model with small static margin. $K_I$ is the integrating-servo gain constant and $K_R$ is the rate-servo gain constant.

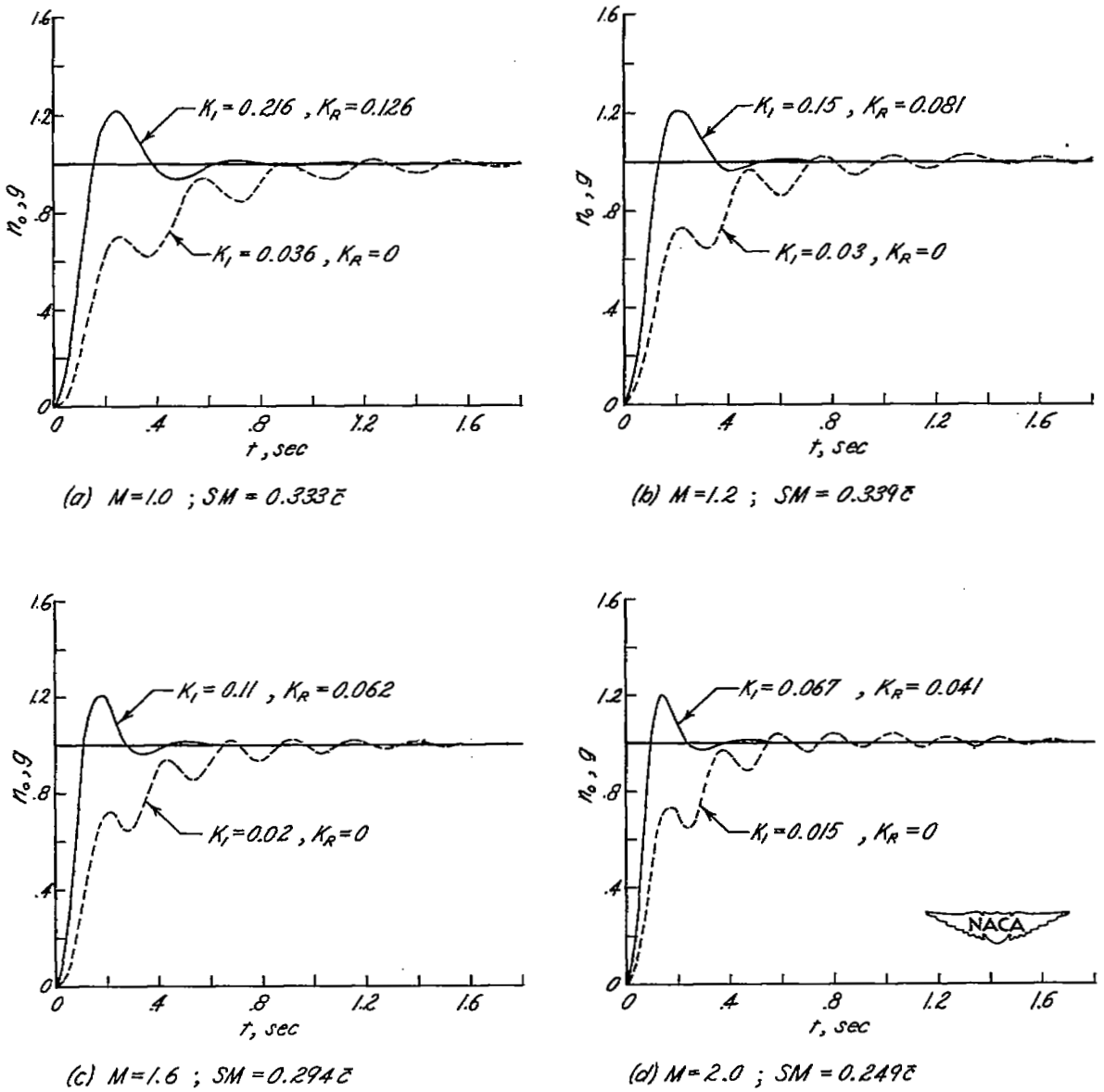


Figure 5.- Normal acceleration ($n_o$) responses to a unit step acceleration input ($n_i$) for various Mach numbers based on sea-level flight of the model with intermediate static margin. $K_I$ is the integrating-servo gain constant and $K_R$ is the rate-servo gain constant.

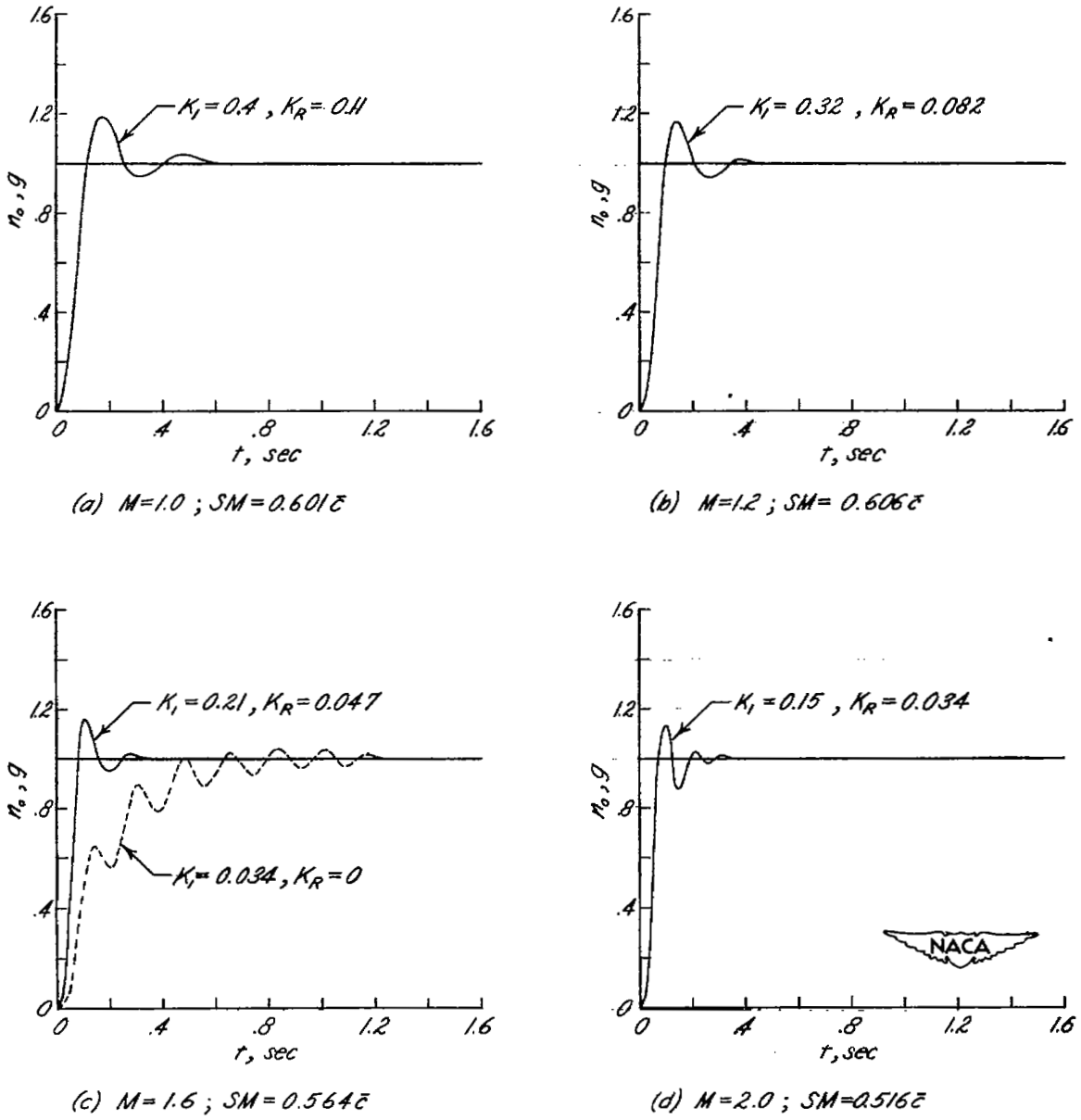


(a) $M = 1.0$ ; $SM = 0.601\bar{c}$

(b) $M = 1.2$ ; $SM = 0.606\bar{c}$

(c) $M = 1.6$ ; $SM = 0.564\bar{c}$

(d) $M = 2.0$ ; $SM = 0.516\bar{c}$

Figure 6.- Normal acceleration ($n_o$) responses to a unit step acceleration input ($n_i$) for various Mach numbers based on sea-level flight of the model with large static margin. $K_I$ is the integrating-servo gain constant and $K_R$ is the rate-servo gain constant.

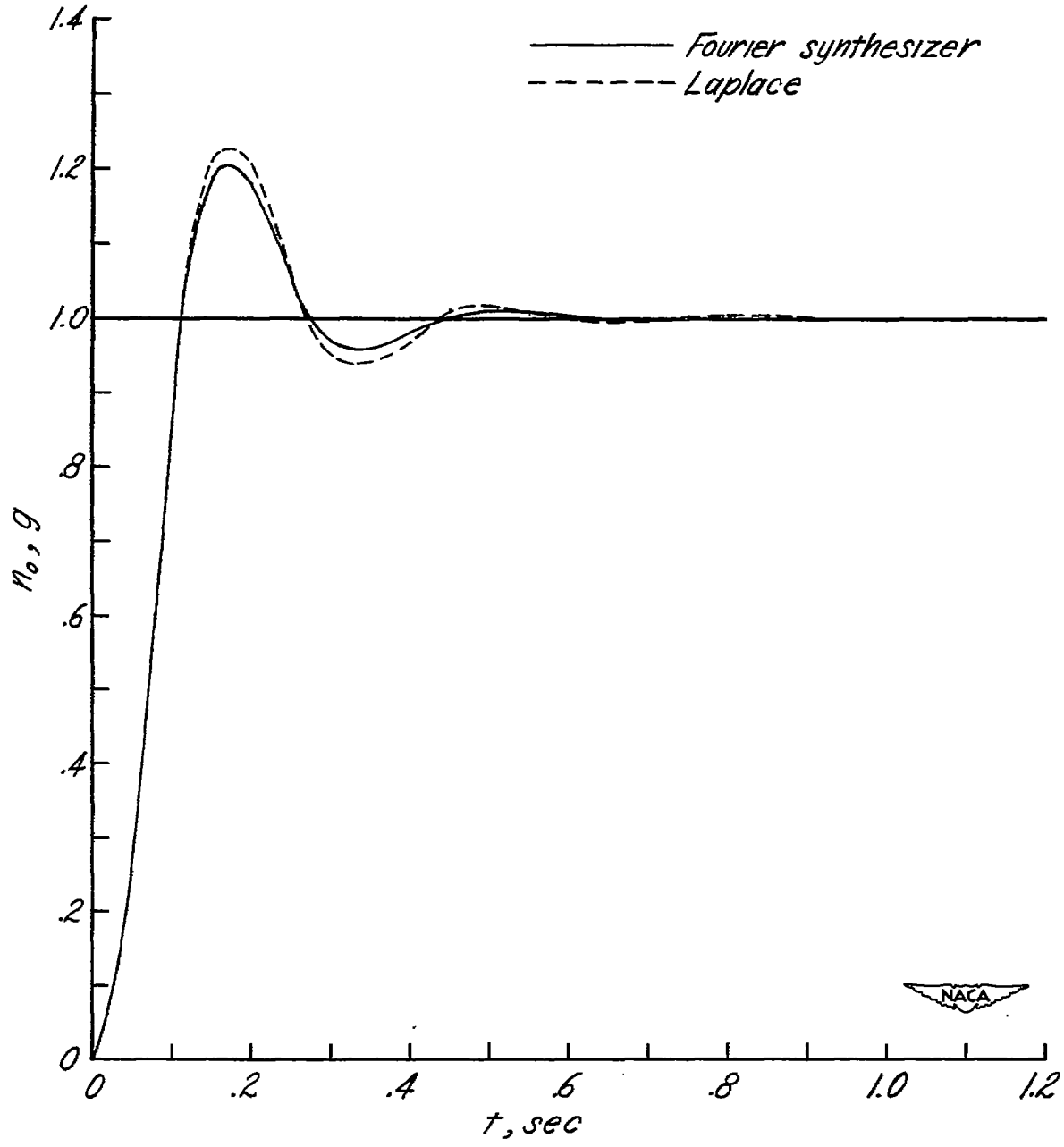


Figure 7.- Comparison of a transient response obtained using the Fourier synthesizer with one obtained using the methods of Laplace. Both curves are based on sea-level flight at $M = 1.6$ and $SM = 0.294\bar{c}$. $K_1 = 0.11$, $K_R = 0.062$.

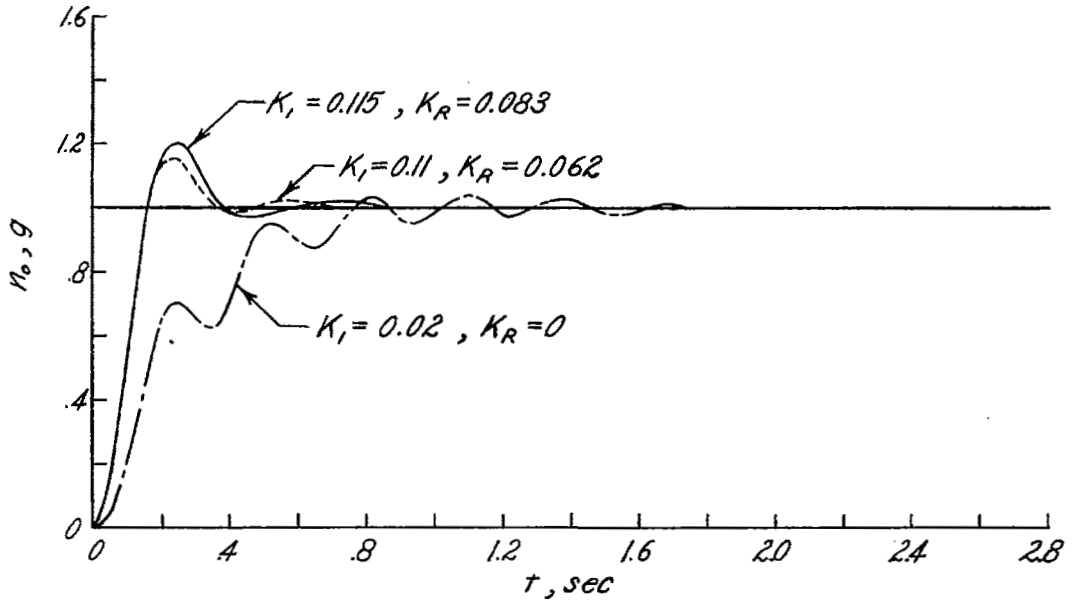


(a) 10,000 feet.

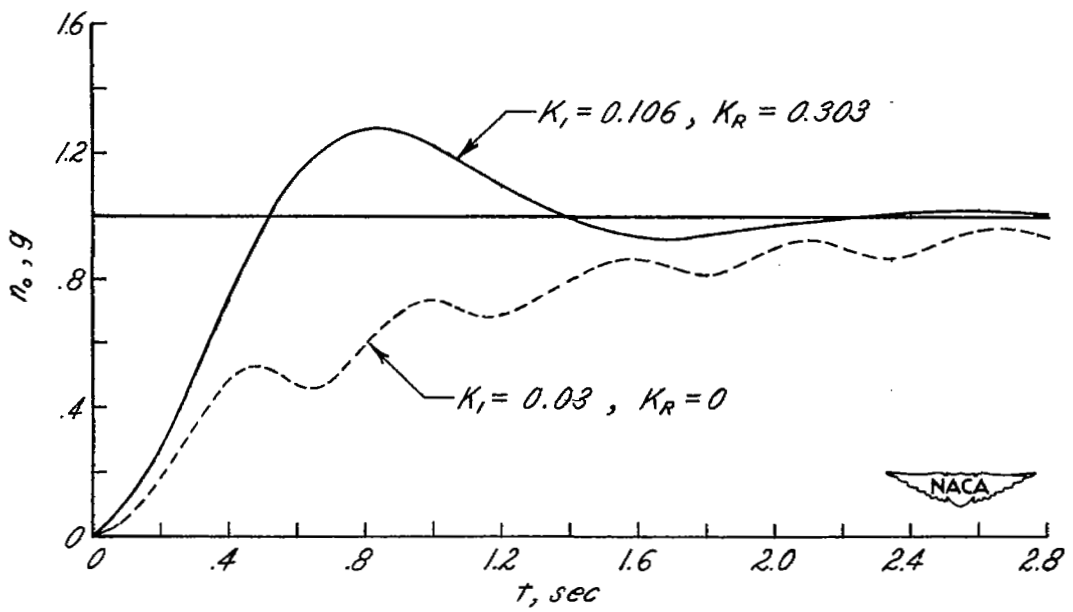


(b) 40,000 feet.

Figure 8.- The effect of flight at altitude on the normal acceleratior ($n_o$) responses to a unit step acceleration input ($n_i$). Responses are based on flight at M = 1.6 and SM = 0.294$\bar{c}$.

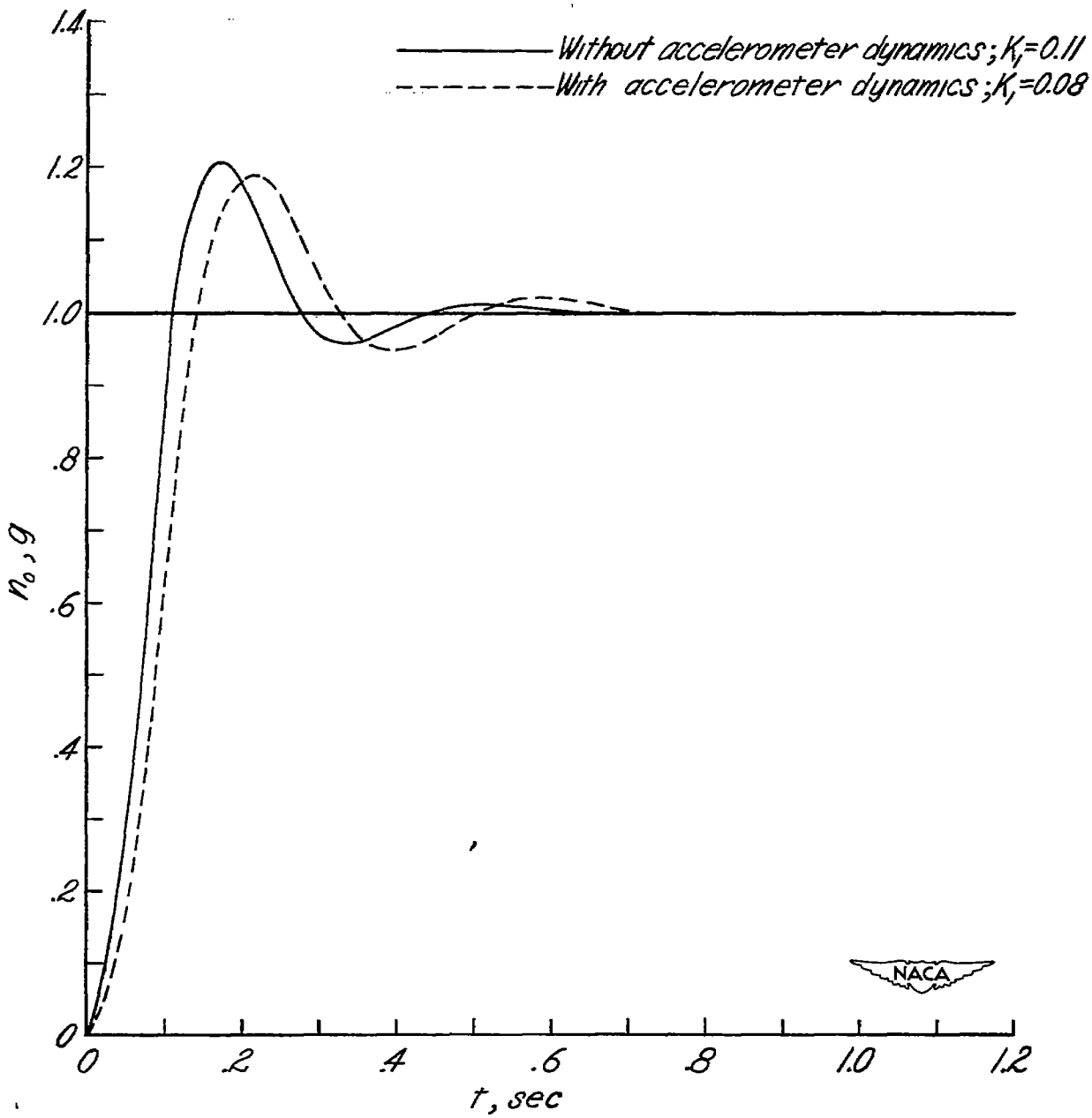


Figure 9.- Comparison of the closed-loop transient responses for the system with and without the dynamics of an accelerometer included in the outer feedback loop. Both curves are based on sea-level flight at $M = 1.6$ and $SM = 0.294\bar{c}$. $(K_R = 0.062)$

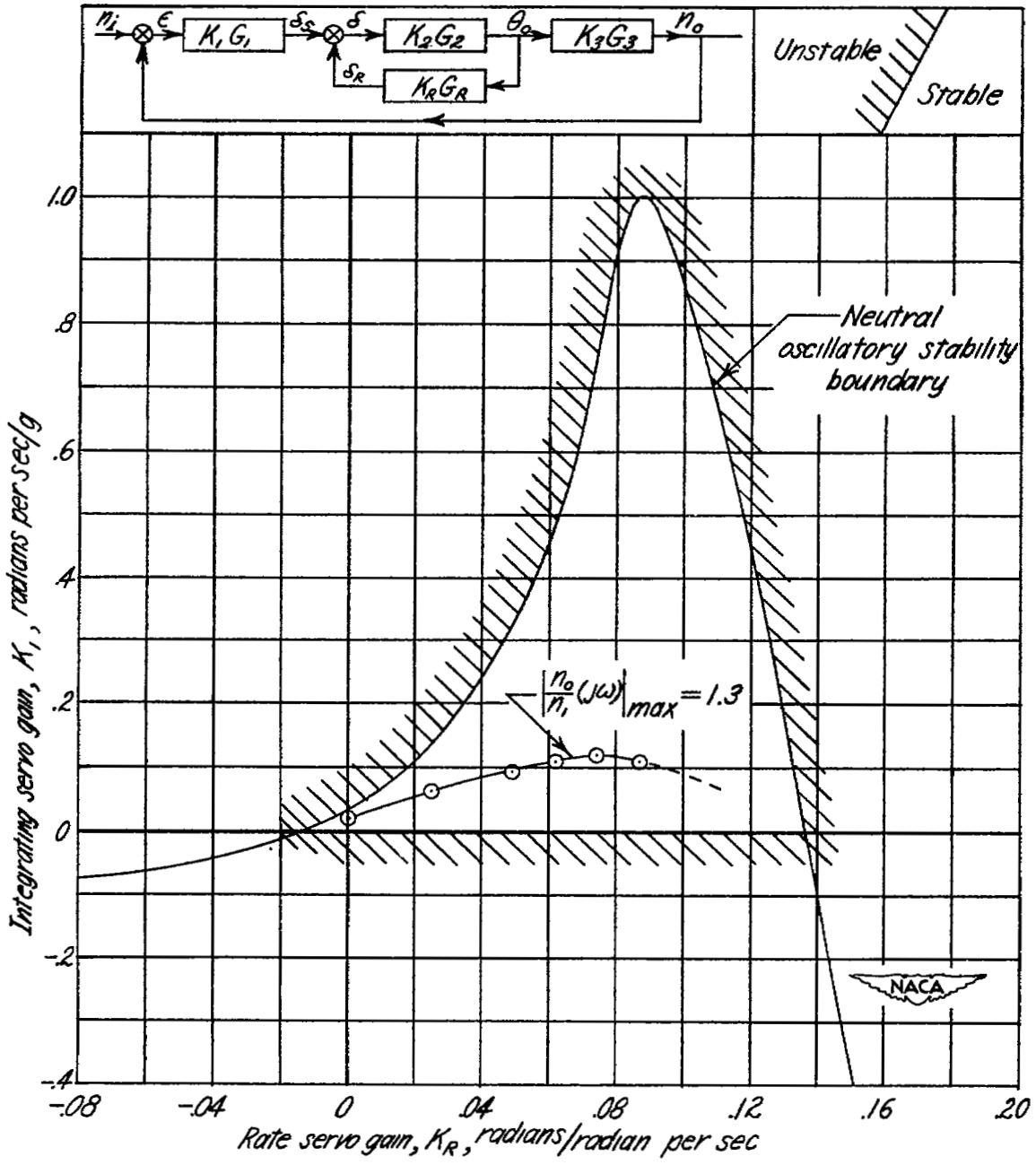


Figure 10.- Application of Routh's discriminant to the characteristic equation of the closed-loop transfer function with the coefficients expressed as a function of $K_I$ and $K_R$ and based on sea-level flight at $M = 1.6$ and $SM = 0.294\bar{c}$.

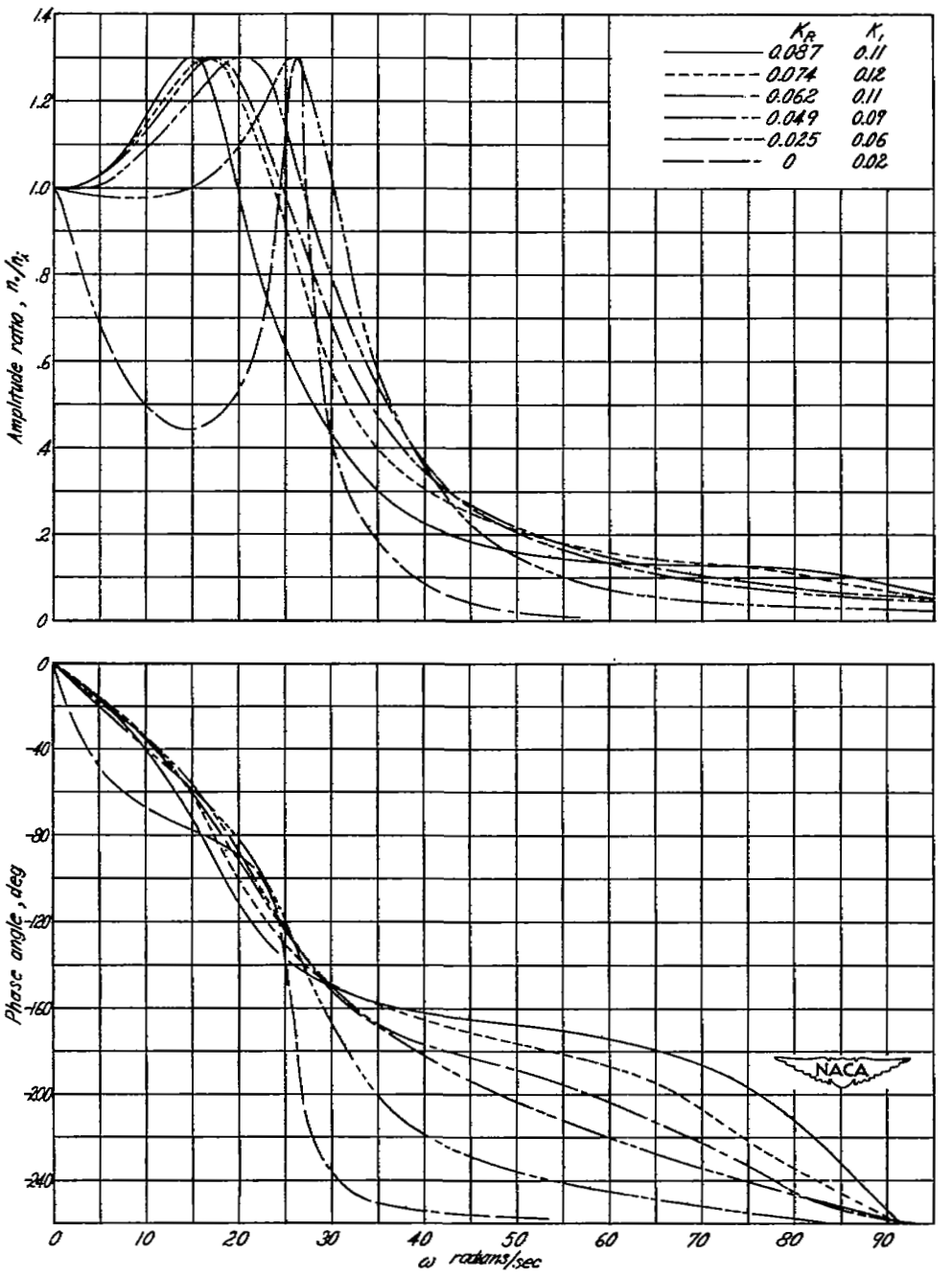


Figure 11.- Closed-loop frequency responses $\left[\frac{n_o}{n_i}(j\omega)\right]$ for various values of $K_R$ and with values of $K_1$ such that the peak amplitude ratio of $\left|\frac{n_o}{n_i}(j\omega)\right| = 1.3$. All responses are based on sea-level flight at $M = 1.6$ and $SM = 0.294\bar{c}$.

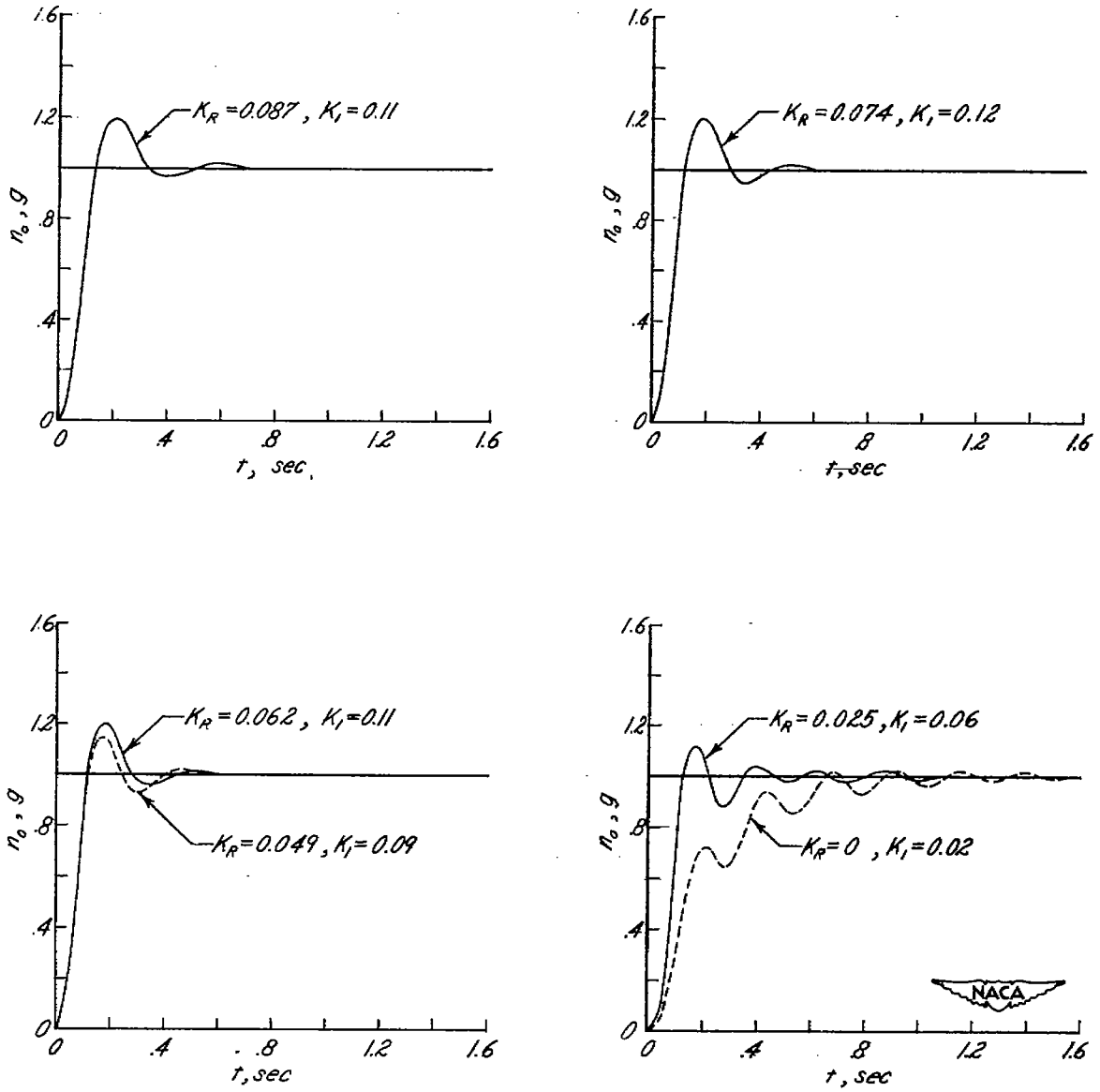


Figure 12.- Normal acceleration ($n_o$) responses to a unit step acceleration input ($n_i$) for various values of $K_R$ and with values of $K_1$ such that the peak amplitude ratio of $\left|\frac{n_o}{n_i}(j\omega)\right| = 1.3$. All responses are based on sea-level flight at $M = 1.6$ and $SM = 0.294\bar{c}$.

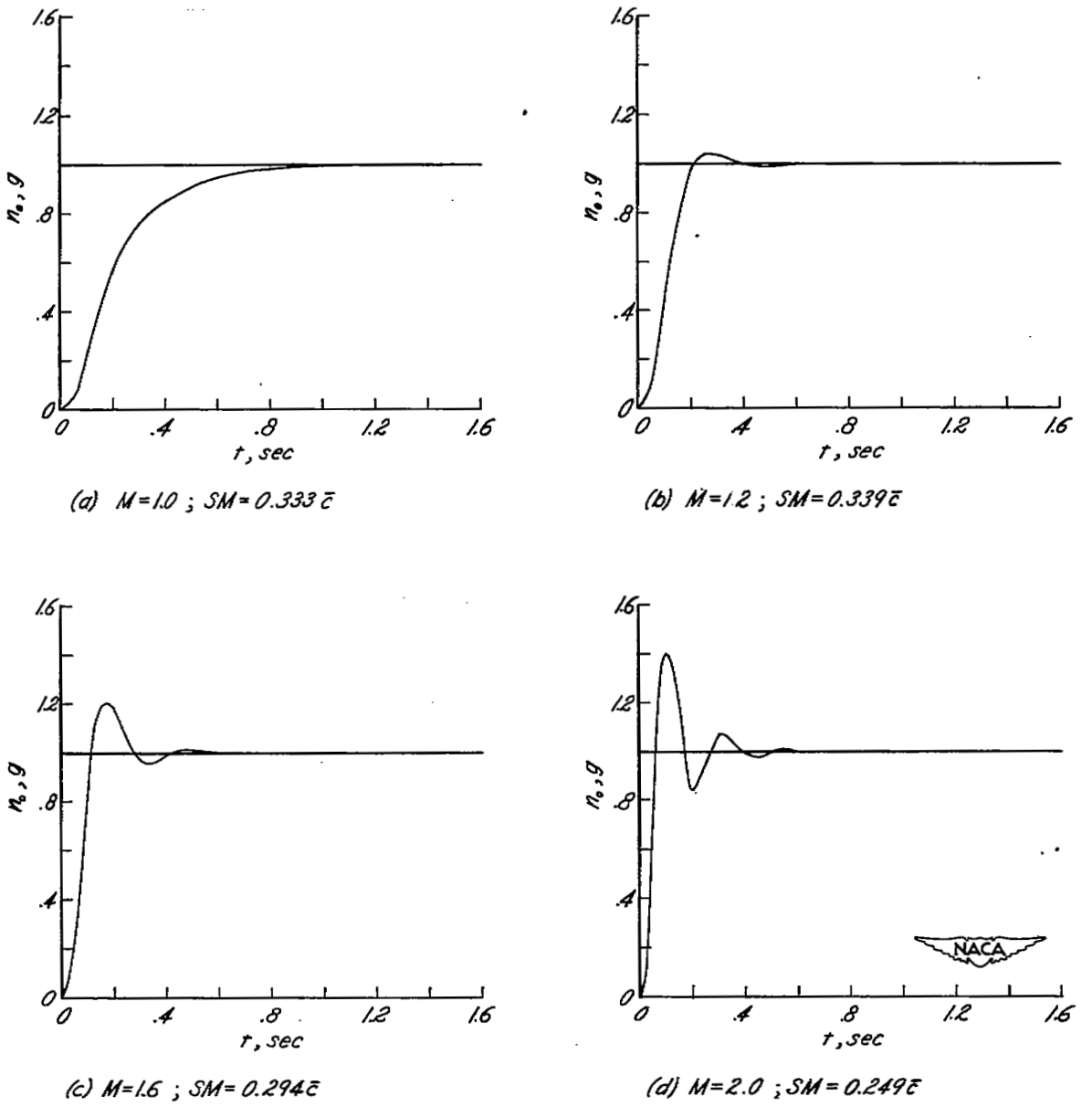


Figure 13.- Normal acceleration ($n_o$) responses to a unit step acceleration input ($n_i$) as obtained for fixed values of integrating- and rate-servo gain constants with Mach number as a variable. Responses are based on sea-level flight of the model with intermediate static margin. $K_I$ = 0.1[illegible] and $K_R$ = 0.062.

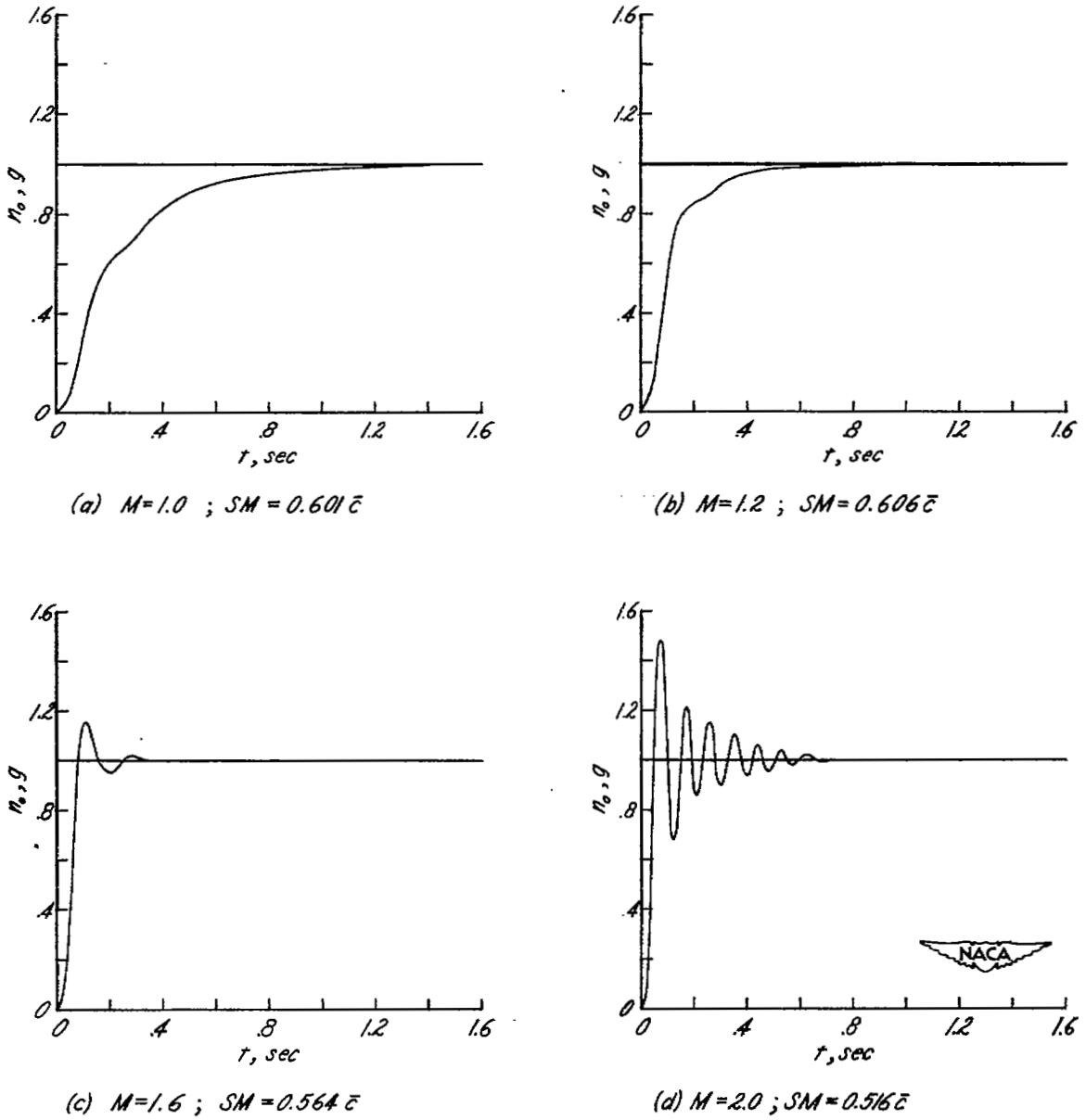


Figure 14.- Normal acceleration ($n_o$) responses to a unit step acceleration input ($n_i$) as obtained for fixed values of integrating- and rate-servo gain constants with Mach number as a variable. Responses are based on sea-level flight of the model with large static margin. $K_I$ = 0.21 and $K_R$ = 0.047.

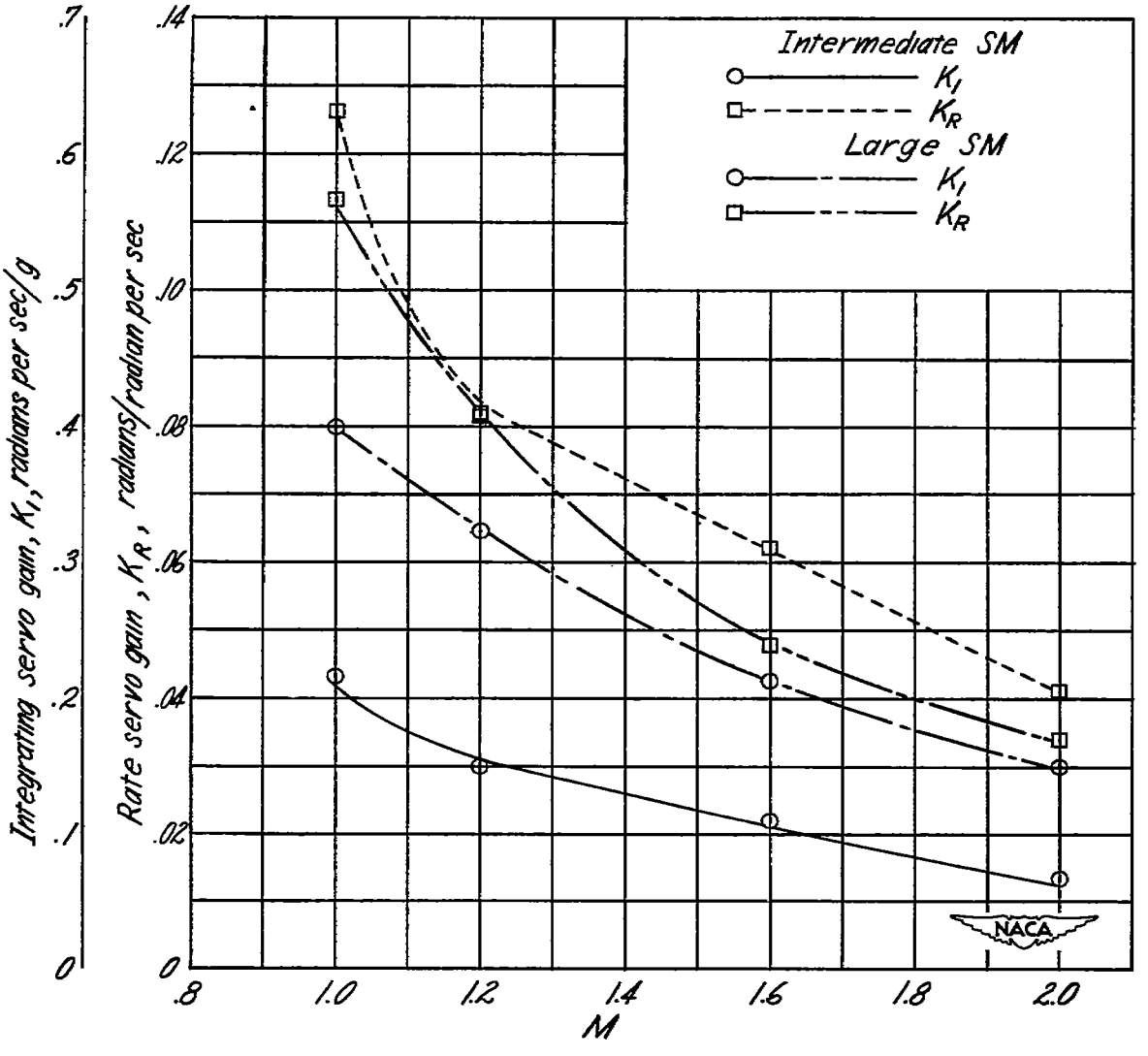


Figure 15.- Variation of $K_I$ and $K_R$ with Mach number when values of $K_I$ are chosen so that $\left|\frac{n_o}{n_i}(j\omega)\right|_{max} = 1.3$ and the values of $K_R$ are chosen so that $\left|\frac{\delta_R}{\delta_S}(j\omega)\right|_{max} = 1.3$.

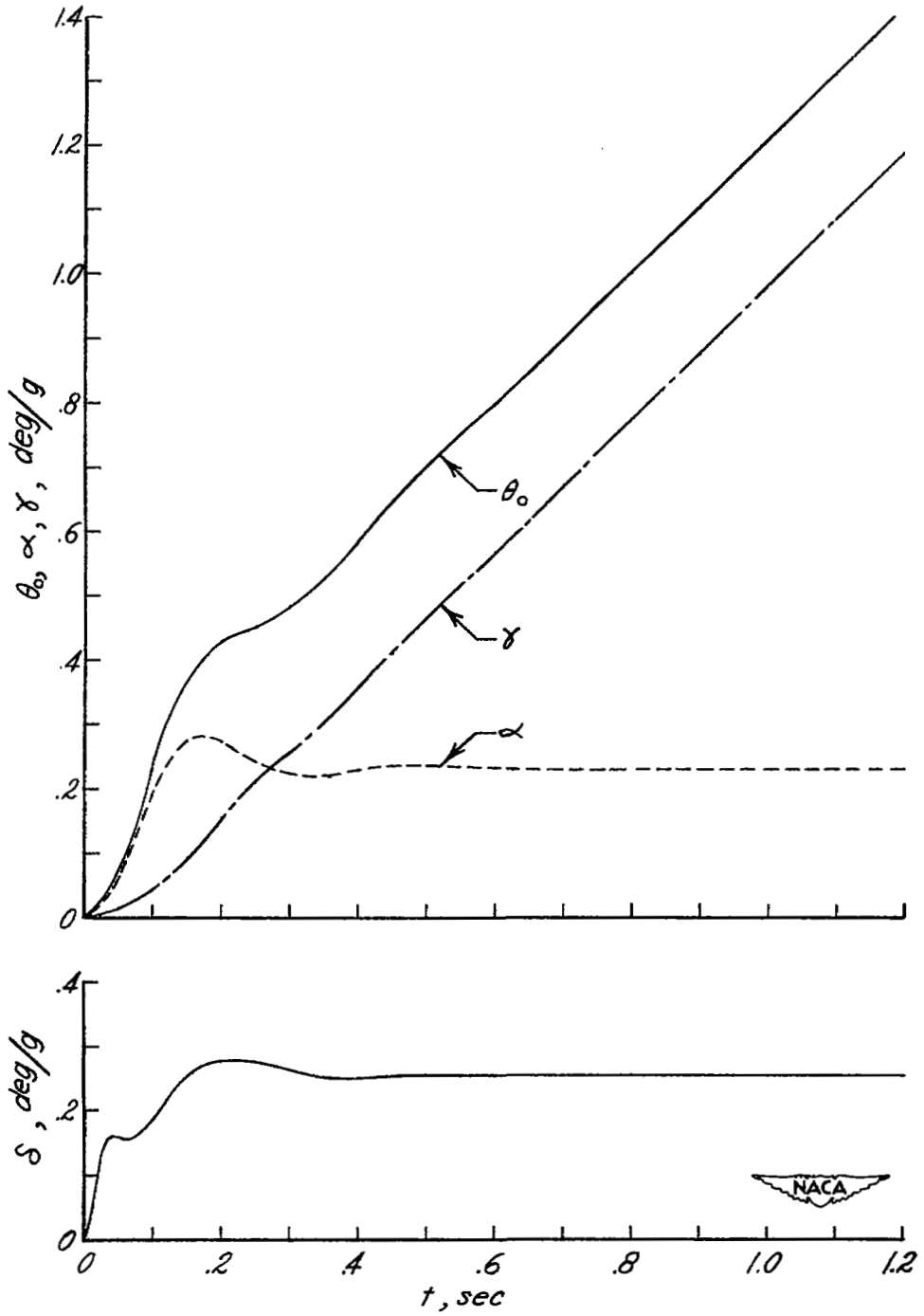


(a) SM = 0.294$\bar{c}$; $K_1$ = 0.11; $K_R$ = 0.062.

Figure 16.- Transient responses of $\theta_o$, $\alpha$, $\gamma$, and $\delta$ to a unit step acceleration input based on sea-level flight at M = 1.6.

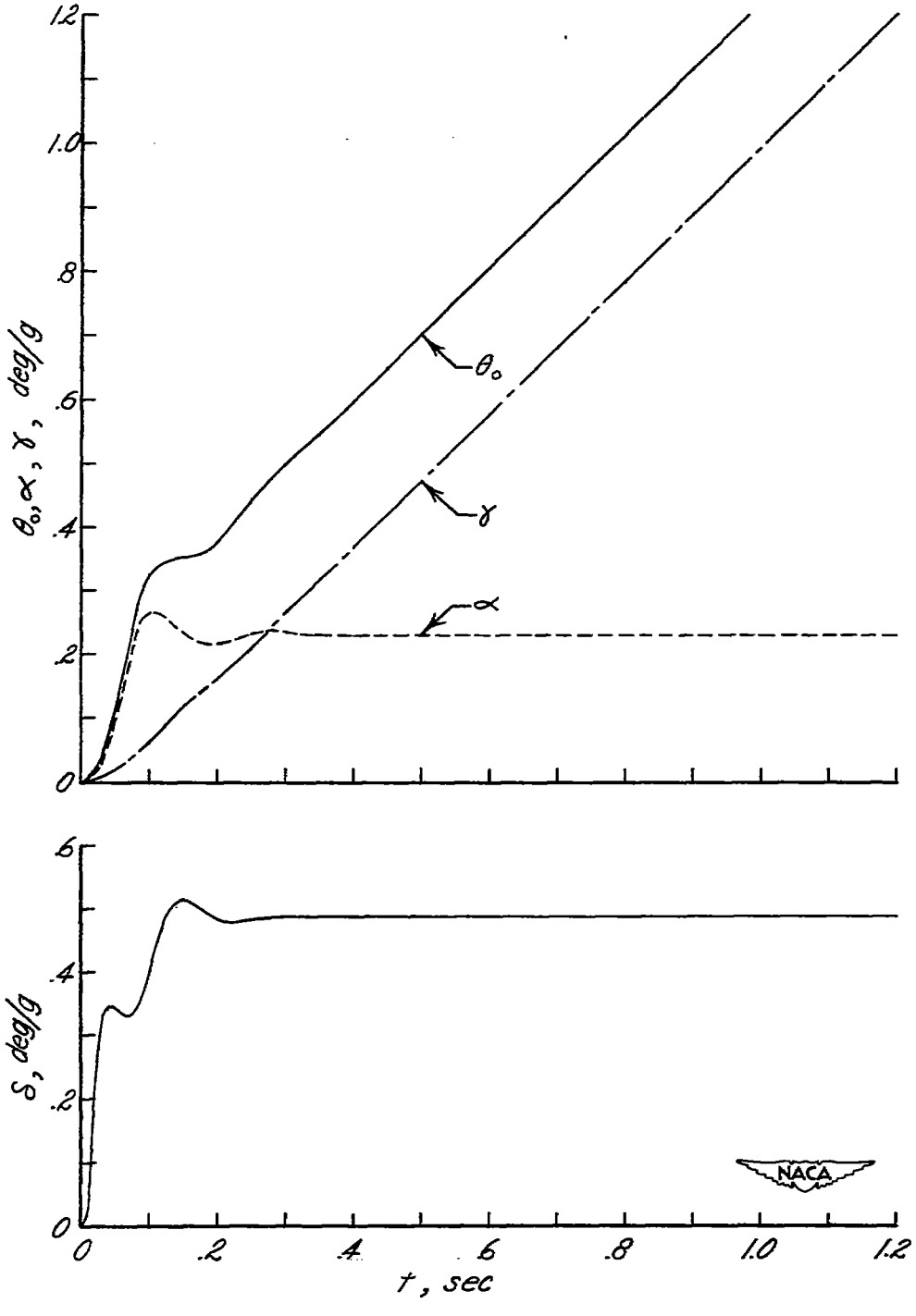


(b) SM = $0.564\bar{c}$; $K_1$ = 0.21; $K_R$ = 0.047.

Figure 16.- Concluded.

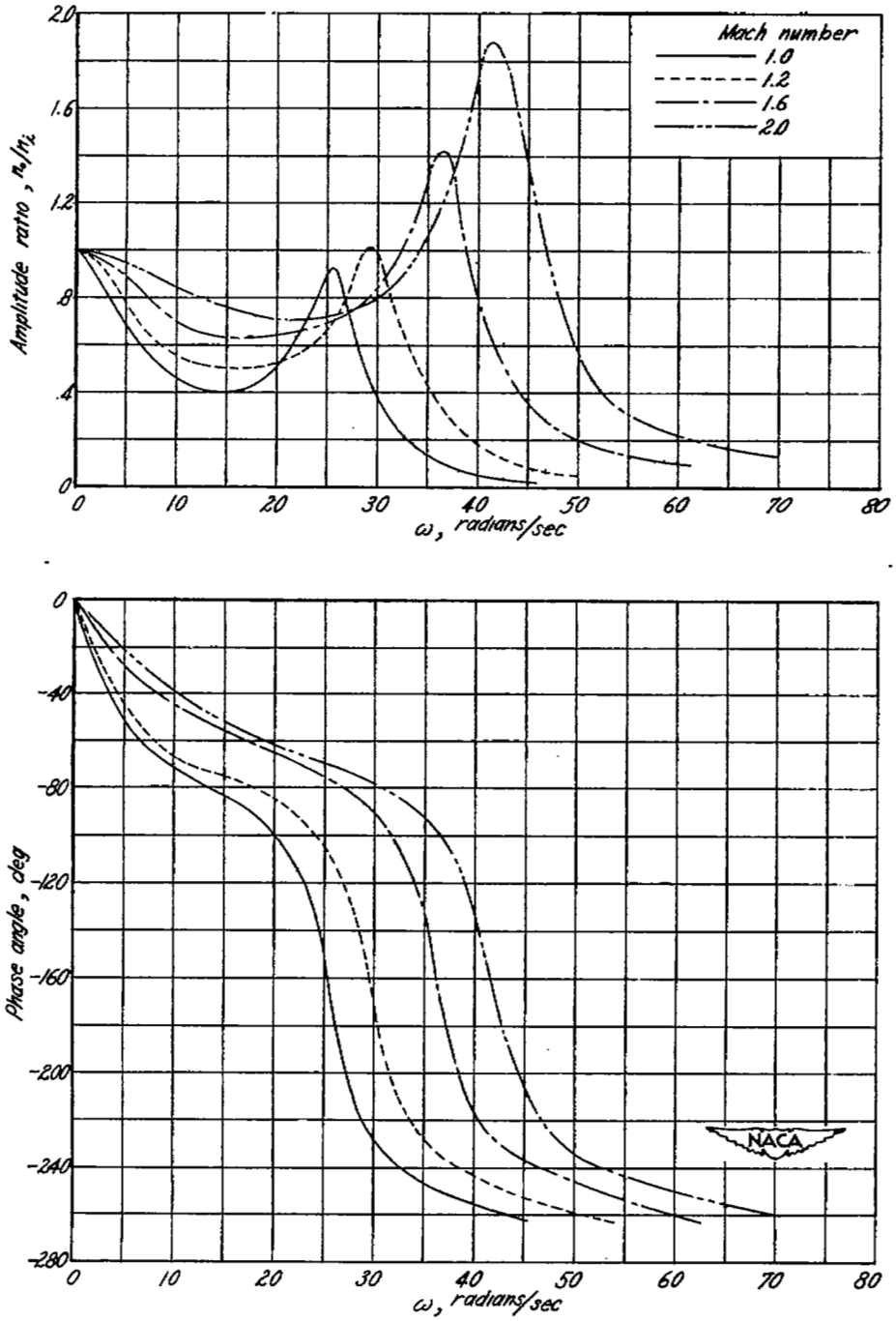


(a) Closed-loop frequency responses $\frac{n_o}{n_i}(j\omega)$.

Figure 17.- System frequency and transient responses obtained for various Mach numbers with an accelerometer placed five feet ahead of the model center of gravity to generate both normal-acceleration error and rate-of-pitch feedback signal. $K_1 = 0.09$; effective $K_R = 0.014$.

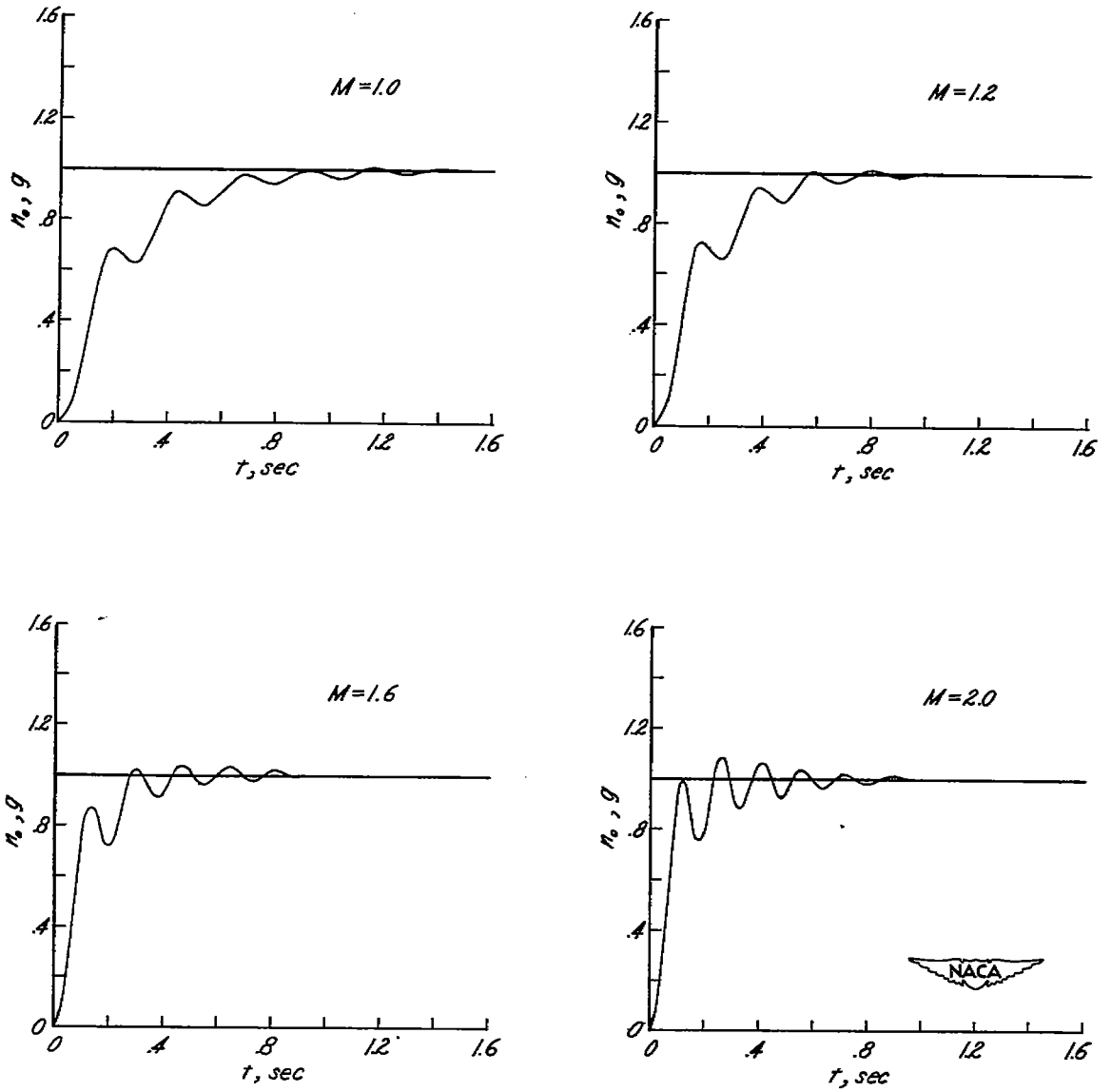


(b) Normal-acceleration ($n_o$) transient responses to a unit step acceleration input ($n_i$).

Figure 17.- Concluded.

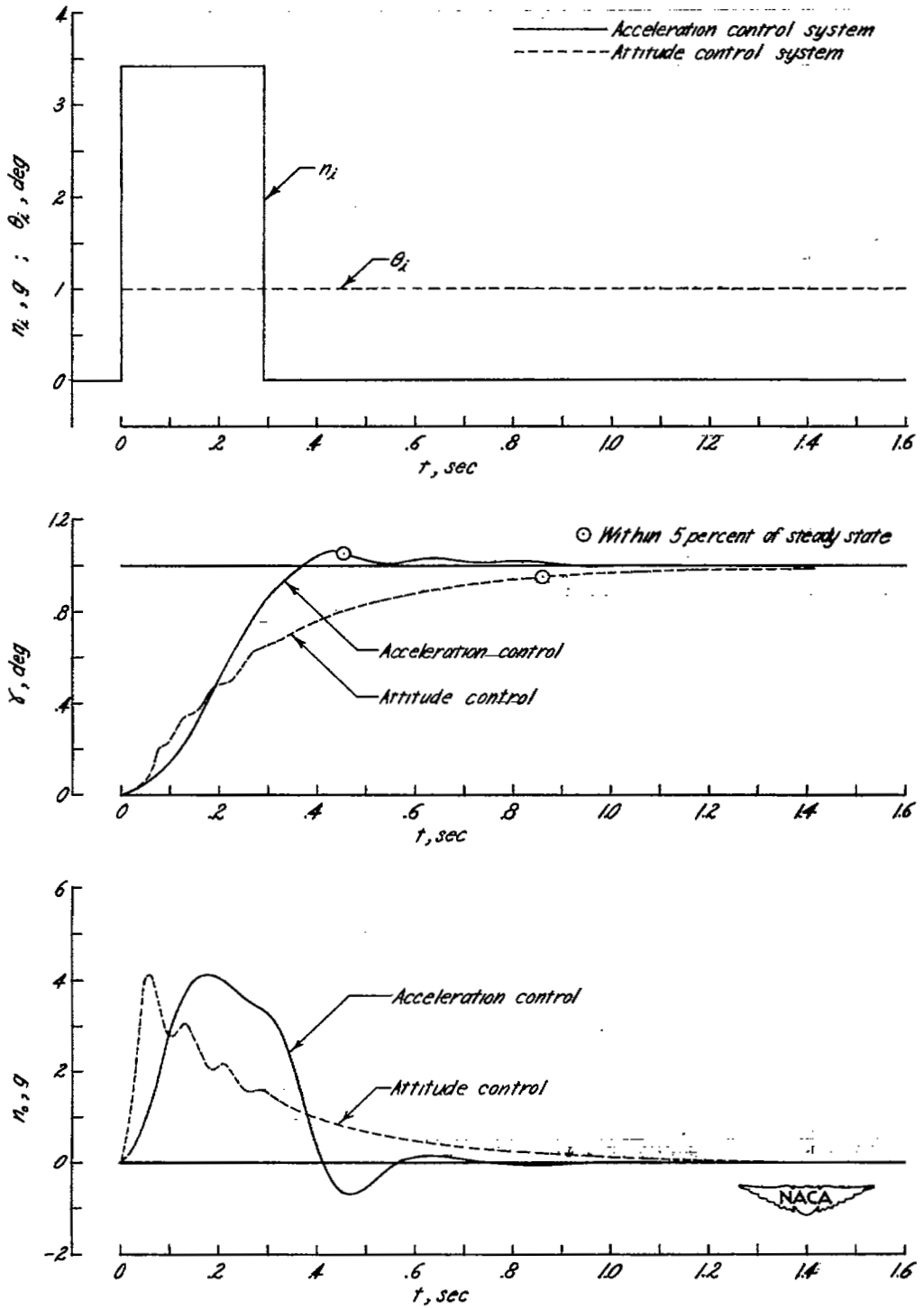


Figure 18.- Comparison of $\gamma$ response times for acceleration control system and attitude control system with equal maximum normal accelerations.

NACA-Langley - 7-10-51 - 385